Intrinsically tuning the electromechanical properties of elastomeric dielectrics: a chemistry perspective

Christopher Ellingford, Christopher Bowen*, Tony McNally, Chaoying Wan*

Christopher Ellingford, Dr. Chaoying Wan, Prof. Tony McNally

International Institute for Nanocomposites Manufacturing (IINM), WMG, University of

Warwick, CV4 7AL, UK;

Email: Chaoying.wan@warwick.ac.uk

Prof. Christopher Bowen

Department of Mechanical Engineering, University of Bath, BA2 2ET, UK

Email: C.R.Bowen@bath.ac.uk

Keywords: Dielectric elastomer; chemical modification; relative permittivity; energy harvesting; actuation.

Abstract

Dielectric elastomers have the capability to be used as transducers for actuation and energy harvesting applications due to their excellent combination of large strain capability (100 ~ 400%), rapid response (10⁻³ s), high energy density (10 ~ 150 kJ·m⁻³), low noise and lightweight nature. However, the dielectric properties of non-polar dielectric elastomers such as dielectric permittivity (ε_r) , breakdown strength (E_b) and dielectric loss (ε') , need to be improved before they can be used effectively in real world applications. The degree of polarity and dielectric properties of non-polar elastomers, such as poly(dimethylsiloxane) and poly(styrene-butadiene-styrene), have often been modified 'extrinsically' by blending with polar polymers or incorporating functional nanoparticles. However, the introduction of polar groups or structures into non-polar dielectric elastomers through covalently bonding is an attractive approach as it can 'intrinsically' induce a permanent polarity to the dielectric elastomers, and can eliminate the poor post-processing issues and breakdown strength of extrinsically modified materials. This review discusses the main chemical methodologies employed to chemically modify dielectric elastomers, namely hydrosilylation, thiol-ene click chemistry, azide click chemistry and atom transfer radical polymerisation. The effects of the type and concentration of polar groups on the dielectric and mechanical properties of the elastomers are analysed in detail and their performance in actuation and harvesting systems are discussed. Current state-of-the-art developments and perspectives of modified dielectric elastomers for deformable energy generators and transducers are provided.

1. Introduction

Electroactive polymers are smart materials that can change shape and size when stimulated by an electric field. Electroactive polymers are classified as either ionic polymers or electronic polymers according to their actuation mechanisms. Ionic polymers respond to an electric field through ion diffusion in gel-like polymers, while the electronic polymers deform by being driven by an electric field or Coulomb forces. The unique electromechanical properties of electronic polymers make them attractive for a wide range of applications in modern power electronic systems such as actuators, generators, electrical motors, vibration-control sensors, self-prime pumps, autofocus lenses, artificial muscles, and variable impedance devices. [1, 2]

1.1 Classification and working mechanism

Figure 1A shows the general classification scheme of electroactive polymers where electronic polymers include dielectric elastomers, ferroelectric polymers, and electrostrictive graft elastomers. Dielectric elastomers are electroactive polymeric network materials that exhibit large strains (100 $^{\sim}$ 400 %) and a fast response (10 $^{-3}$ s) upon application of an electric field, and can transduce mechanical energy into electricity or *vice versa*. They typically require a large actuation voltage (500 $^{\sim}$ 10 kV)^[3] due to their need to

operate at high electric fields, but at low electrical power consumption due to the low current. Ferroelectric polymers are semi-crystalline thermoplastic polymers, such as polyvinylidene fluoride (PVDF), which relies on the polarisation and orientation of polar crystal phases to convert mechanical or thermal energy into electricity.

The working mechanisms of the two types of electroactive polymers as generators are compared in **Figure 1 B** and **C**. For the ferroelectric polymers the remnant polarisation leads to bound charge which can be harvested due to the application of an applied stress which modulates the polarisation level. The piezoelectric effect in PVDF semi-crystalline polymer stems from the polarisation and charge distribution in the VDF repeating unit. For the dielectric elastomers, the absence of a remnant polarisation requires a different mode of operation, which will now be described by considering the electrical and mechanical energy in a polymeric electro-mechanical system.

1.2 Electrical storage in a polymer capacitor

The capacitance (C) of a parallel plate capacitor is proportional to the dielectric permittivity (ε) and surface area (A), and reciprocal to the thickness (d) of the dielectric, as expressed by **Equation 1**. The amount of stored electrical energy, W for polymer-based capacitors can be expressed as **Equation 2**, which is related to the dielectric permittivity (or relative permittivity, ε_r) and breakdown strength (E_b) of the dielectric.

$$C = \varepsilon_0 \varepsilon_r \frac{A}{d} \tag{1}$$

$$W = 0.5CV^2 = 0.5\varepsilon_r \varepsilon_0 A dE_b^2 \tag{2}$$

The key electrical properties required for dielectric materials in electrical power applications include the breakdown strength, relative permittivity and dielectric loss. Many polymers are considered unsuitable for dielectric-related applications due to their intrinsically low permittivity ($\varepsilon_r = 2^{\sim}10$) and low energy density ($U_e = 1^{\sim}3$ J·cm⁻³), although their dielectric

loss and breakdown strength ($E_b > 500$ MV/m) are typically higher than most dielectric ceramic materials.

1.3 Mechanical to electrical energy conversion in polymers

Dielectric elastomers and ferroelectric polymers behave differently for energy harvesting and transduction. As shown in Figure 1B, the working mechanism of dielectric elastomer generators includes a four-step cycle. It is firstly elastically deformed to increase the mechanical elastic energy and increase the capacitance C of the elastomer by increasing the area (A) and reducing the thickness (d). Next, an applied voltage leads to charges (Q) at the interface between the dielectric elastomer and the compliant electrodes. The dielectric elastomer in then unloaded in step 3, reducing the elastic energy stored which leads to a reduction in area and increase in thickness. Due to the resulting reduction in capacitance, there is an increase in voltage, according to Q = CV, and an increase in electrical energy, according to $W = 0.5CV^2$. The final step discharges the electrical energy from the material, thereby harvesting the increased energy. [4,5] Key requirements for dielectric elastomers for energy generation therefore include a high permittivity to maximise the stored charge for a given operating voltage and high breakdown strength to maximise the operating voltage. [6, 7] The materials must also be able to be highly deformable with a large elastic strain to provide large and recoverable changes in area, thickness and capacitance. A low dielectric loss (typically a dissipation factor of tan δ < 0.05) is also essential for efficient energy transduction within a system.

In comparison, the piezoelectric effect in PVDF semi-crystalline polymer stems from the polarisation and charge distribution in the VDF repeating unit and the different crystal phases. The orientation of the β -phases under the external force increases the polarisation

level and surface charge. When an alternating stress is applied to the piezoelectric, it generates an AC current through the load impedance (Figure 1C). [8]

Various strategies have been explored to improve the electromechanical performance of dielectric polymers. A recent review has comprehensively overviewed the effects of chemical modification on the properties of electroactive fluorinated polymers. [9] The orientation polarization is regarded as an effective approach to increase the dielectric constant of ferroelectric PVDF and its copolymers, and the dielectric loss can be mitigated by a multilayer film assembly. [7] The working mechanisms and configurations of ferroelectric polymer nanocomposites for energy harvesting and storage have been discussed in detail by Wan et al^[8] and recently by Gupta et al.^[10] Modification of dielectric elastomers, with a focus on silicone-based transducers $^{[3]}$ and actuators $^{[11,\ 12]}$ have been overviewed and the correlation of molecular structure and properties of silicone elastomers for stretchable actuator applications has discussed. [2] The development of various dielectric elastomers including acrylates, silicones, polyurethanes and the compliant electrodes have been critically commented. [13] The applications of dielectric elastomers for electronic muscles and skins, [14] acoustics and vibration control, [15] soft robotics [16] have also been overviewed. As demonstrated in the previous research, the electromechanical properties of dielectric elastomers can be improved by constructing inhomogeneous structures through the incorporation of high-permittivity ceramic nanoparticles or electrically conducting metallic or carbonaceous nanomaterials. [17, 18] However, this approach of developing extrinsically enhanced materials has met with technical challenges, including dispersion/aggregation, interface incompatibility, selection/optimisation of different particles with different polymer matrices, as well as the complex effects of post-treatment on the structure and electromechanical performance such as pre-strain, thermal annealing, shape-recovery rate

and hysteresis.^[8] In addition, the enhanced dielectric constant and energy density of polymer dielectrics are often at the expense of increased dielectric loss, and compromised breakdown strength, mechanical properties and processability.^[19]

The chemical design and covalent modification of dielectric elastomers enables additional dipole moments to be permanently attached to the polymer network structure, which intrinsically tunes the dielectric properties of the polymers. However, there are limited studies on chemical modification of dielectrics due to the limited information on the available organic dipoles and dipole properties, multi-step chemistry processes and high cost. It is therefore timely to overview the current status of chemical modification of dielectric elastomers and shed light on the development direction towards flexible and stretchable electromechanical energy harvesting and storage devices, touch sensors, actuators or field-effect transistors. In this review, the working mechanism of dielectric elastomers is firstly summarised and the critical structure parameters of elastomers are introduced. Four main chemical methods for modification of elastomers are overviewed. The relationships between the structures of the modified elastomers and their electromechanical properties and applications are discussed.

2. Structure and properties of dielectric elastomers

Dielectric elastomers are electroactive, can change shape upon being electrically charged, and exhibit muscle-like actuation or transduction, as well as energy generation during deformation - a reversal of the energy input into the dielectric elastomers for actuation purposes.

Table 1 shows the electrical and mechanical properties of a range of dielectric elastomers poly(styrene-butadiene-styrene) (SBS), poly(styrene-ethylene-butadiene-styrene) (SEBS), poly(dimethylsiloxane) (PDMS) and ethylene-propylene-diene monomer rubber (EPDM) and

(BaTiO₃) and lead zirconium titanate (PZT). The electrical properties of permittivity, loss and breakdown strength are shown along with the mechanical properties of strength, stiffness and strain to failure. The d_{33} in Table 1 is the piezoelectric coefficient and represents the induced strain in the poling direction (z-direction) per unit of applied electric field in the zdirection or charge per unit applied force and applies to only the ferroelectric materials. Dielectric elastomers have a three-dimensional lightly crosslinked network structure, which generally possess higher mechanical flexibility than semicrystalline PVDF-based polymers, enabling large elastic deformations for flexible and deformable energy harvesting applications. [22, 23] The macromolecular structures of selected dielectric polymers are shown in Figure 2. The breakdown strength for SBS and PDMS are high, see Table 1, with a similar value to PZT and PVDF, showing their potential advantages compared to ferroelectric materials. However, it is clear that the relative permittivity of all dielectric elastomers are significantly lower than both PVDF and piezoelectric ceramics and the dielectric elastomers do not exhibit a piezoelectric coefficient since they have no remnant polarisation which means that their change in capacitance with loading must be used for energy harvesting, as in Figure 1B.

their comparison to semicrystalline PVDF and ferroelectric ceramics such as barium titanate

There are three main challenges that dielectric elastomers must overcome:

- 1. improvement of ε_r to increase the potential difference generated upon mechanical deformation with a low dielectric loss (ε') to prevent loss of energy;
- 2. achieving a high electrical breakdown strength (E_b) to prevent electrically induced failure and maximise the operating electric field;
- 3. achieving a high tensile strength (T), a high elongation at break (λ_{max}), and a low stiffness (Y).

For practical applications, Madsen et al pointed out that the dielectric elastomers should possess properties of $\varepsilon_r \ge 10$, $\tan \delta \le 5\%$, T > 2 MPa, $\lambda_{max} > 200\%$, $Y \sim 1$ MPa, and $E_b > 50$ V μm^{-1} to allow the materials to deform easily with a large extensibility and achieve a high energy density. However, this combination of properties is difficult to achieve since targeting the improvement of the relative permittivity tends to result in less favourable mechanical properties and a reduction in the breakdown strength or increased dielectric loss. [3]

To compare different dielectric materials, relevant figures of merit can be used for actuation and energy generation principals as shown in **Equation 3** and **4**. For dielectric elastomer actuation, the figure on merit below stems from the actuation strain equation in section 5,

Figure of Merit (actuation) =
$$\frac{3\varepsilon_0\varepsilon_r E_b^2}{\gamma}$$
 (3)

For dielectric elastomers for energy generation, a modified version of the McKay Figure of Merit is used where the strain energy function of the elastomer is assumed to be a constant, as shown in Equation 4, [31]

Figure of Merit (generation) =
$$\varepsilon_0 \varepsilon_r E_b^2$$
 (4)

where Equation 4 is a similar to the figure of merit for energy storage in a capacitor, Equation 2, although for a generator a high strain to failure is also necessary. These Figure of Merit values are normalised against that of PVDF and shown in Table 1 since it represents a material with high permittivity and breakdown field, making it of interest for capacitor applications.^[10]

1. Extrinsic approaches to improve the dielectric properties of elastomers

The properties of dielectric elastomers can be improved extrinsically via (i) blending of different polymers to combine their advantageous properties and (ii) addition of high-permittivity or conducting nanoparticles to dielectric elastomers. Furthermore, the

performance of dielectric elastomers can also be tailored by configurational design of the devices at multi-scale levels. For example, a multi-layered structure enhances the dielectric performance of dielectric films through either alternatively stacking different types of polymer layers, from insulting/electrically conducting to semi-crystalline polymer/elastomer, or tailoring the layer thickness and interface. As such, there are a large variety of different configurations available to use with dielectric elastomers including rolled, trench and spider modes to accommodate different applications, see **Figure 4**. [39]

Figure 3 provides an overview of the modification methods for electromechanical properties of dielectric polymers. The blending of polar polymers is an effective approach for enhancing both the dielectric permittivity and the electrical breakdown strength compared to the neat/pure polymers. The intermolecular interactions exhibited between polar groups is the underlying reason, and results in an increase in the energy density of the material, which is of interest for energy harvesting applications. For example, as seen in **Table 2**, the blending of PVDF and P(VDF-TrFE-CFE) at 40/60 vol% resulted in a ε_r = 38 and an enhanced E_b = 640 V μ m⁻¹ leading to U_e = 19.6 J cm⁻³. [40] Once again, the Figure of Merit values have been normalised to PVDF for comparison. **Figure 5a** shows how the dielectric permittivity and electrical breakdown strength changes depending on the material used and the resulting effect of modification on these materials. Both the dielectric permittivity and electrical breakdown strength contribute to the energy density of a material – the amount of energy that can be stored within it. **Figure 5b** shows that Young's modulus is a material dependent property, rather than being linked to the relative permittivity.

The combination of high-permittivity ceramic particles such as BaTiO₃, ^[50, 51] PZT, ZrO₂ ^[52] with relative a permittivity in excess of $\varepsilon_r = 1000^{[53]}$ or electrically conducting nanoparticles such as graphene^[54] and carbon nanotubes, ^[55] with dielectric elastomers has been considered to

generate extrinsically enhanced polymer composites with increased dielectric properties. [8] However, the large difference in relative permittivity and surface energy between the particles and polymer matrices only results in moderate enhancement of the dielectric properties of the composites, and is accompanied by a reduction in breakdown strength [3, 56] and mechanical flexibility, [57] as well as large dielectric loss [56] due to interfacial defects. [58] The interfacial compatibility between inorganic particles in a polymer matrix can be improved through surface modification of the fillers. This can be achieved by attaching polymer brushes onto the particle surfaces via 'grafting to' or 'grafting from' approaches, or forming core-shell structured particles, as summarised in **Figure 6**. Thermally expanded graphene sheets have been mechanically mixed into PDMS with a weight fraction of up to 2 wt%, which increased the relative permittivity of PDMS from $\varepsilon_r = 3$ to $\varepsilon_r = 11$ at 2 wt% of graphene, and stress at 100% strain from 0.33 MPa to 0.99 MPa. However, this led to a tan $\delta = 1$ which was an increase by two orders of magnitude. [59]

Both dopamine and silane surface modification on BaTiO₃ and TiO₂ was investigated in silicone rubber and nitrile-butadiene rubber (NBR) matrices respectively. The modified BaTiO₃ nanoparticles showed strong interfacial interactions with the silicone, leading to an improved dispersion. This results in an increase in the relative permittivity compared to the unmodified siloxane, whilst maintaining the level of dielectric loss, a decrease in the Young's modulus and an increase in the breakdown strength. [50] A similar result was observed with regard to the properties of ε_r , ε' , γ and ε_b for the surface modification of TiO₂ by increasing the compatibility of the nanoparticles with the NBR matrix. [60]

Therefore, the formation of composite materials using conducting fillers such as polyaniline (PANI), carbon nanotubes and graphene have shown to be a promising approach for permittivity enhancement. However, the concentration of the conducting fillers should be

maintained below the *percolation threshold*, otherwise a conductive pathway is formed through the polymer matrix. As a result of forming a conductive network, the capacitor/insulator relationship in dielectric elastomers is lost and both the ε_r and ε' increase significantly, see **Figure 7**. [61] Therefore the addition of a filler close to the percolation threshold is desirable for maximum ε_r enhancement, although this is also likely to increase the electric field. [19] When incorporating carbon nanotubes, a percolation threshold as low as 0.07 wt% has been reported. [62]

The percolation threshold and the observed dielectric permittivity are related by Equation 5,

$$\varepsilon_{eff} = \varepsilon_m \left(\frac{\Phi_c}{\Phi_c - \Phi} \right)^s$$
 (5)

where ε_{eff} is the effective dielectric permittivity, ε_m is the dielectric permittivity of the polymer matrix, Φ_c is the percolation threshold, Φ is the volume fraction of conducting filler added and s is a constant greater than zero. [63]

Early work involved PANI particles that were encapsulated in poly(divinylbenzene) using miniemulsion polymerisation and then added into PDMS. This allowed the PANI particles to become charged under an electric field and enhance the dielectric properties, whilst not forming a conducting network. This increased the relative permittivity of the material from $\varepsilon_r = 2.3$ to $\varepsilon_r = 7.6$ at 100 Hz with a 31.7 vol% loading. [64]

A different approach has been to chemically modify PANI with hyperbranched poly(siloxane) through a ring opening polymerisation. This was mixed with thermally reduced graphene where it interacted through π - π interactions. The thermally reduced graphene had a good compatibility and dispersion in an acrylic resin elastomer as the poly(siloxane) was able to hydrogen bond with the acrylic resin elastomer. Overall, the use of chemically modified

PANI and thermally reduced graphene in acrylic resin elastomer resulted in a relative permittivity of ε_r = 350 and a loss of ε' = 0.37 at 100 Hz. [65]

4. Intrinsically tuned electromechanical properties of dielectric elastomers

Non-polar polymers exhibit two forms of polarisation, which arise from electronic polarisation and atomic polarisation. Electronic polarisation originates from the displacement of the electron cloud around an atom. This results in shifting the atomic nuclei from the centre of the cloud and leads to a permittivity of $\varepsilon_r \sim 2$. The effect of electronic polarisation is relatively small as the intra-atomic field is stronger than an applied electronic field, reducing the distortion of the electronic cloud. [66] Atomic polarisation is caused by the distortion of the atomic nuclei arrangement in the polymer. The origins of this polarisation is from bond bending and stretching and typically has an intensity of 10% relative to the electronic polarisation. [66]

Chemical modification of elastomers by covalently introducing polar groups to the polymer backbone can permanently change the structures and intrinsically tune the electromechanical properties. This is a result of an increase in the level of atomic polarisation increasing as the difference between the positive and negative centres on the polymer chains grows larger. This also introduces the potential for orientation polarisation in which permanent dipoles align with an applied electric field, see **Figure 8**. However, only a few at any one time will align with the electric field since overcoming the potential energy barrier to movement, caused by molecular and electrostatic interactions, does not guarantee alignment as there are multiple different orientations possible. In addition, random thermal motion contributes to a reduction in polarisation. The overall polarisation is the sum of the polarisation from electronic, atomic and orientation effects.

Further orientation of polar groups can be achieved by drawing a polymer uniaxially or by annealing of the polymer. [67]

The dielectric permittivity of a material and its dipole moment are related by the molar polarisation equation in **Equation 6** $^{[68]}$

$$\frac{\varepsilon_r - 1}{\varepsilon_r + 2} = \frac{\rho N_A}{3M\varepsilon_0} \left(\alpha + \frac{\mu^2}{3kT} \right) \tag{6}$$

where ε_r is the dielectric constant, ρ is the mass density, N_A is Avogadro's number, M is the molar mass, ε_0 is the permittivity of a vacuum, α is the polarisability, μ is the dipole moment, k is the Boltzmann constant and T is the absolute temperature. This shows that increasing the polarisation and dipole moment of a dielectric elastomer can increase the relative permittivity of the material.

Chemical modification of elastomers affect the properties from two aspects. Firstly, grafting of polar or electron-withdrawing side groups to the polymer backbone can increase the dipole moment and increase the dielectric constant; $^{[43, 44, 68]}$ and increasing the size of grafted side groups such as using bulky groups can increase the free volume of the polymer, thus providing more space for polar groups to align with an electric field and increase the ε_r , By increasing the grafted side chain length, the chain entanglement density can be altered, thus reducing the Young's modulus of the material without affecting the electrical breakdown strength which is of benefit to achieve a high energy density and actuation strain. $^{[69]}$

Secondly, increasing the crosslinking density within a dielectric material can help to 'lock' polar groups into a single orientation and prevent their free movement to introduce a common directionality for polarity across the entire structure, which improves the electrical properties. In addition, introducing crosslinking alters the physical properties of the polymer from a viscous gel into a solid crosslinked polymer, and thus increased the

strength.^[2] However, the introducing polar groups to elastomers can also increase its water sensitivity and glass transition temperature (T_a) .^[72, 73]

Research into this area is still in its infancy. Four key reaction methods have been used to modify elastomers, i.e., hydrosilylation, thiol-ene click chemistry, azide click chemistry and atom transfer radical polymerisation (ATRP), as shown in **Figure 9**. The reaction conditions and effects of modification on the dielectric properties of elastomers are now discussed.

4.1. Hydrosilylation

Hydrosilylation chemical grafting reactions are typically carried out with silicone-based elastomers, primarily poly(dimethylsiloxane) (PDMS) or poly(methylhydridesiloxane) (PHMS) where Si-H bonds are added across a vinyl group, see **Figure 10**.^[74] A non-functionalised silicone-based elastomer has a relative permittivity of $\varepsilon_r = 2.3 \sim 2.8^{[75]}$ and a breakdown strength of approximately $E_b = 80 \text{ V} \cdot \mu\text{m}^{-1}$. A significant number of organic molecules have been grafted to siloxane chains including ethers, ^[76] esters, ^[76] epoxides, ^[76, 77] carbonates, ^[78] amines ^[76] and aromatic rings, ^[79] although no dielectric data has been reported for these modifications.

Typical reaction conditions for hydrosilylation involve reacting PHMS with a vinyl terminated organic molecule using Karstedt's catalyst under an inert atmosphere, due to the water sensitivity of the reaction. The reactions are heated to 70 $^{\circ}$ 100 $^{\circ}$ C and left to react for between 4 and 22 hours. [27, 80] Thin films are formed by evaporation of the solvent on a non-stick surface and crosslinking is achieved by heating to a high temperature for less than an hour. [27] Due to the requirement for an inert atmosphere and dry conditions during the hydrosilylation step of film formation, there is an increase in complexity and cost in carrying out the reaction for large-scale synthesis compared to other reaction methodologies. The reported thicknesses of the thin films are typically between 100 $^{\circ}$ 150 μ m. [81, 82]

Table 3 summarises work undertaken to date to graft cyano, chloro and trifluoropropyl groups to siloxane-based elastomers. On increasing the grafting level of allyl cyanide, the relative permittivity increases from $\varepsilon_r = 2.5$ for PDMS to $\varepsilon_r = 4.2$ when 8.0 mol% of allyl cyanide is grafted^[82] and up to $\varepsilon_r = 15.9$ when 89 mol% is grafted.^[83] Increasing the grafting of allyl cyanide indicates a near-linear relationship with ε_r , see **Figure 11**. Interestingly there is a greater variation between the results at a low allyl cyanide grafting level compared to the grafting content at higher levels. Potential reasons for this are: small fluctuations in the reported and actual grafting level of organic molecules in the siloxane structures; differences in water content present within the elastomers;^[82] different film thicknesses when testing the dielectric properties and a lack of results at high grafting concentrations for allyl cyanide. The crosslinking has no significant effects on the dielectric properties of the elastomers.^[84]

However, an increased allyl cyanide content resulted in a significantly increased ε' whereby it increased from $\varepsilon' = 2.0 \times 10^{-4}$ for PDMS to $\varepsilon' = 2.5$ at 89 mol% grafting (HS1). This demonstrates that to produce an elastomer for harvesting and actuator applications, the choice of grafted dipole is important to ensure that it results in a desired increase in relative permittivity with minimal effect on the dielectric loss.

Allyl cyanide modified PHMS was added to PDMS as a filler (HS4),^[27] and allyl cyanide was grafted to PHMS-co-PDMS (HS5)^[86] in an effort to improve the mechanical and electrical properties without reducing the relative permittivity of the material. CNATS-993 acted as a plasticiser when used as a filler in HS4, see **Figure 12**, which resulted in an elastomer with a lower *Y* than PDMS. The elastomer had a relative permittivity of $\varepsilon_r = 7.0$ and a low loss of $\varepsilon' = 0.1$, but the breakdown strength was only $E_b = 20 \text{ V } \mu\text{m}^{-1}$ compared to $E_b = 80 \text{ V } \mu\text{m}^{-1}$ for PDMS.^[27]

PHMS with 89 mol% grafting of allyl cyanide was grafted with PDMS in a 1:2 ratio, thus reducing the dipole content to 5.3 wt% (HS5). The relative permittivity was reduced from ε_r = 15.9 to ε_r = 4.9 and resulted in a soft elastomer with a strength of T = 0.49 MPa and a low breakdown strength of E_b = 29 V μm^{-1} . In this work, the reference PDMS material had a strength of T = 3.20 MPa and a breakdown strength of E_b = 49 V μm^{-1} , [86] indicating that sections with a high density of cyanopropyl groups significantly disrupted the structure of the elastomer, as the cyanopropyl groups were not distributed evenly.

Allyl chloride has also been grafted using hydrosilylation. 16.1 mol% of allyl chloride was grafted to PHMS-g-PDMS (HS6), resulting in a permittivity of ε_r = 4.7 and a low loss of ε' = 4.5x10⁻³.^[81] Chloro groups are less polar than cyano groups^[87] and thus the reported relative permittivity of ε_r = 4.7 is only marginally greater than the relative permittivity of ε_r = 4.2 for 8.0 mol% grafting for HS2, as polarity is the main factor for an increase in relative permittivity.^[82] The breakdown strength remained high at E_b = 94.4 V μ m⁻¹, and the elastomer remained strong and elastic with T = 2 MPa, Y = 1 MPa and λ_{max} = 130%. ^[81] With these properties, the Figure of Merit for actuation is 11 times higher than PVDF. It is therefore feasible that a higher doping level of allyl chloride could result in a greater relative permittivity than previously reported, and result in better enhancement for actuation.

The ability to maintain the mechanical properties originated from the ability of the chloropropyl molecules to provide 'self-lubrication.', where the chloropropyl groups reduce the intermolecular chain frictional forces due to an increase in the free volume in the matrix.^[88]

Incorporating 57.5 mol% of trifluoropropyl into PDMS (HS7a) increased the relative permittivity to $\varepsilon_r = 6.4$, which is comparable to a 23.0 mol% grafting level of cyanopropyl groups in the elastomer (HS3). The dielectric loss of the system was two orders of

magnitude lower than the incorporation of trifluoropropyl, demonstrating that this modification produced a silicone elastomer with improved dielectric properties.

Changing the group between chloro and trifluoropropyl does not appear to have a major effect on the permittivity, despite an increase in polarity. The lowest level of trifluoropropyl grafted was 28 mol% which resulted in $\varepsilon_r = 5.1$. Conversely, when only 16 mol% of allyl chloride was grafted the permittivity remained similar, with $\varepsilon_r = 4.7$. [81]

The mechanical properties of HS7a have been significantly reduced with a low strength and stiffness reported of T=0.05 MPa and Y=0.018 MPa respectively, producing a gel-like elastomer. Reducing the grafting level to 52.9 mol% (HS7b) did not significantly affect the dielectric properties of the material, but doubled the strength to T=0.13 MPa with a doubling of λ_{max} and a similar elasticity to HS7a. Whilst this was an improvement, the elastomer remained too weak to use in energy harvesting applications, as the desired strength is $T \simeq 2$ MPa according to Madsen *et al.* This also demonstrates that the use of chloro groups instead of trifluoro groups should potentially be preferred for use in future elastomer systems.

Grafting N-allyl-N-methyl-p-nitroaniline to different siloxane chains, including 'off-the-shelf' PDMS, was investigated to determine how the dielectric properties were influenced, see **Table 4**. N-allyl-N-methyl-p-nitroaniline is readily described as a 'push-pull' dipole, increasing compatibility with the silicone matrix owing to homogenous incorporation into the elastomer matrix.^[89]

PDMS DMS-V31 and DMS-V41, with molar masses of 28000 g mol⁻¹ and 62700 g mol⁻¹ respectively, were grafted with N-allyl-N-methyl-p-nitroaniline to determine the impact of the dipole and PDMS chain length on dielectric properties. The highest grafting concentration, 13.4 wt% of N-allyl-N-methyl-p-nitroaniline, led to the highest permittivity

for both elastomers with ε_r = 5.98 for DMS-V31 and ε_r = 5.40 for DMS-V41. However by incorporating this dipole, the ε' for each elastomer increased by an order of magnitude with respect to the unmodified siloxane chains. [89, 90]

DMS-V31 has a shorter chain length compared to DMS-V41, and thus has a greater crosslinking density. The impact of this is seen in the tensile strength of DMS-V31 compared to DMS-V41 despite 13.4 wt% of N-allyl-N-methyl-p-nitroaniline being grafted. However, the dipole affects the elastic properties of both elastomers, with the Young's modulus of DMS-V31 decreasing from Y=1.7 MPa to 0.3 MPa and for DMS-V41 decreasing from 0.95 MPa to 0.25 MPa. This demonstrates that the increased crosslinking density has a minimal impact on Young's modulus, unlike its effect on tensile strength, and that the grafted dipole is the key factor for increased elasticity. As expected, increasing the grafted dipole concentration decreased the dielectric strength from $E_b=130$ V μ m⁻¹ and 80 V μ m⁻¹ to $E_b=40$ V μ m⁻¹ and 30 V μ m⁻¹ for DMS-V31 and DMS-V41 respectively. [89, 90]

Elastosil RT625 and Sylgard 184 were also investigated in the same manner with N-allyl-N-methyl-p-nitroaniline, both with a grafting degree of 10.7 wt%. Despite a lower grafting degree, the relative permittivity for Elastosil RT625 (ε_r = 5.56) was between DMS-V31 (ε_r = 5.98) and DMS-V41 (ε_r = 5.40), whereas for Sylgard 184 the relative permittivity was higher (ε_r = 6.15). Both of these modified elastomers were mechanically weaker with tensile strengths of 0.1 MPa and 0.5 MPa respectively. This implies the Elastosil RT625 elastomer is too weak for energy harvesting applications, but the material had the highest Figure of Merit values for actuation. However, while the Sylgard 184 elastomer was relatively weak, it also had the highest Young's modulus of 0.85 MPa. [91] This, coupled with the relatively high dielectric strength and high permittivity, means it is one of the best off-the-shelf PDMS candidates for further modification and is reflected in the high Figure of Merit values for

energy generation. However, the low strength is a disadvantage. Blending of Sylgard 184 and DMS-V31 has the potential to produce an elastomer that has both good electrical and mechanical properties when modified.

The effect of polarity from the grafting of different functional groups to siloxane chains has been investigated by Racles *et al.* to determine if there is a direct correlation between the dipole moment of the side chain group and its permittivity. [82] Allyl aldehyde, allyl glycidyl ether, 4-amino pyridine, allyl cyanide and disperse red 1 were grafted to PHMS-*g*-PDMS at an 8 mol% doping level using hydrosilylation, whilst chloropropane-thiol and 3-mercaptopropionic acid were grafted using thiol-ene click chemistry (see section 4.2 for more detail on thiol-ene click reactions) using vinyl modified siloxane chains (PVMS-*g*-PDMS); see **Table 5**. The dipole moments for the grafted organic dipoles were calculated using Density Functional Theory (DFT) and Molecular Mechanics. [82]

The general trend observed was that an increase in the dipole moment of the grafted organic molecule increased the permittivity. The lowest polarity molecule resulted in a relative permittivity of ε_r = 3.8, which increased to ε_r = 7.4 when higher polarity groups were grafted. However, only a weak correlation was found, as can be seen in **Figure 13**. Some of the elastomers displayed an unexpectedly high permittivity if it is assumed that the permittivity was dependant only on the dipole moment. The dipole moment of polar group disperse red 1 is 10.40 Debye (D) with the modified elastomer exhibiting a permittivity of ε_r = 5.4, whereas 4-aminopryidine had a dipole moment of 5.67 D but showed a higher permittivity of ε_r = 7.4. A similar disagreement towards the general trend is observed between allyl glycidyl ether and chloropropane-thiol. Both have a similar relative permittivity of ε_r = 3.8 but a different dipole moment, 2.19 D and 3.22 D respectively. [82] This indicates other factors aside from polarity affect the dielectric properties for the modified

elastomers which arises from a combination of steric factors and water sorption of the organic dipoles, as the ions from water can affect conductivity and dielectric properties. [92] The effect of this is further seen in the differences in ε' between 4-aminopyridine and disperse red 1. The dielectric loss for disperse red 1 is ε' = 0.22, but rises greatly to ε' = 5.9 for 4-aminopyridine. [82] Therefore, 4-aminopyridine modified elastomers are unsuitable for energy-transducing and actuator applications due to their high dielectric loss. However, elastomers grafted with disperse red 1 could be a suitable candidate for further research. An interesting adaptation to the modification of PDMS is to form an elastomer with polar organic groups on the crosslinker instead of on the main chain. Several ready modified crosslinkers can be bought and used directly to form elastomers, removing an entire synthetic procedure and overcoming the challenges from hydrosilylation as the water sensitivity element of the reaction is negated. However, the maximum achievable degree of grafting is significantly lower than chemical modification of the elastomer backbone. [93] The effect of various different organic groups have been studied including methyl, phenyl, chloropropyl, aminopropyl and cyanopropyl in addition to the length of the PDMS chains used in the elastomers from 34500 g mol⁻¹ (A) to 125000 g mol⁻¹ (B). [93] The results summarised in Table 6 show that with both chain lengths of PDMS, grafting cyanopropyl groups to the crosslinker resulted in the largest increase in relative permittivity for the chains, with ε_r = 3.7 for PDMS A and ε_r = 3.3 for PDMS B. This result was unsurprising, as cyanopropyl had the highest dipole moment of all the organic groups. The incorporation of a low polarity methyl group yielded the lowest permittivity, ε_r = 2.5. One surprise was that addition of the chloropropyl group resulted in a smaller increase in permittivity than the aminopropyl group, despite the greater polarity of chloropropyl. [93] This was attributed to the increase in free volume from the larger size of the chloro group. [93] However, water

sorption investigations were not carried out, preventing the impact of water ions on the dielectric properties of the elastomers being assessed.

The elastomers formed for both PDMS chain lengths of A and B generally had poor mechanical properties. Using crosslinkers modified with phenyl and cyanopropyl with PDMS chains A only resulted in the best mechanical properties with a strength of T=1.2 MPa and Y=0.68 MPa for A-phenyl and a strength of T=2.1 MPa and Y=0.95 MPa for A-cyanopropyl. The increased strength of the elastomers when the shorter PDMS chain length of A was used is likely due to the increased crosslinker density in the elastomer. However, the difference between cyanopropyl and phenyl modified crosslinkers compared to the methyl, chloropropyl and aminopropyl modified crosslinkers is likely due to inter and intramolecular interactions arising from the addition of the cyanopropyl group, or additionally π - π stacking between the phenyl modified crosslinkers. Therefore, chemical modification of future elastomers could involve both grafting to the chain and to the crosslinker, assuming the crosslinker will increase the strength of the material instead of disrupting the structure.

4.2. Thiol-ene click chemistry

Thiol-ene click grafting reactions can be carried out on any elastomers in which a vinyl group is present, such as SBS or poly(vinylmethylsiloxane) (PVMS), through S-H bond addition across the double bond, shown in **Figure 14**. Typically, unmodified SBS has a permittivity of $\varepsilon_r = 3.90$ and a high breakdown strength of $E_b = 65$ V μ m⁻¹.^[24] Typical reaction conditions for modification of elastomers involve dissolving a photoinitiator such as 2,2-dimethoxy-2-phenylacetophenone (DMPA), elastomer and organic molecule in a solvent and irradiation of the solution with UV light. The reaction is carried out without the need for an inert

atmosphere, unless the organic molecule is at risk of becoming oxidised.^[94] The grafting level for thiol-ene click chemistry is determined by how long the solution is exposed to UV light to induce the reaction, making the modification easily controlled.

A number of different polar groups have been grafted to butadiene-based polymers including mercaptan groups with amine, [95, 96] carboxylic acid, [95-97] ester [96, 97] and cyclic ether functionalities. [95, 97] However, little work has been undertaken to investigate the dielectric properties of the elastomers. The use of click chemistry for chemical modification of elastomers is desirable for industrial applications due to its simple reaction procedures, ease of purification, high product yields and short reaction times, see **Figure 15**.

Methyl thioglycolate and thioglycolic acid, which are similar sized groups but with an ester and carboxylic acid functionality respectively, were grafted to SBS; see **Table 7**. Grafting 83 mol% of thioglycolic acid resulted in an increase in the permittivity of SBS from ε_r = 2.2 to ε_r = 7.2, with a low dielectric loss of ε' = 0.3 (TC2). [94] Grafting methyl thioglycolate to SBS also resulted in an elastomer with significantly improved dielectric properties, with an increased relative permittivity of ε_r = 12.2 and a reduced loss of ε' = 0.07 (TC1). [24] Therefore using an ester group has a more desirable effect on the dielectric properties compared to the carboxylic acid. The fall in the dielectric loss for the ester group is possibly due to a lower water sorption ability of the elastomer from the increased hydrophobicity of the grafted group.

The mechanical properties of the two elastomers are also different. The ester modified SBS has a high strength, with a strength of T=3 MPa whilst also having a good elasticity with Y=0.34 MPa and $\lambda_{max}=1400\%$. However, for the carboxylic acid modified SBS the mechanical properties are relatively poor. The material has a lower strength, T=1.1 MPa, and the elastomer is less flexible and less ductile as Y=3.3 MPa and $\lambda_{max}=300\%$. [94] From

these results, modification of SBS with an ester group results in an elastomer with superior properties than a carboxylic acid modified SBS elastomer. However, the breakdown strength for both elastomers was relatively low, $E_b = 15.7 \text{ V } \mu\text{m}^{-1}$ for ester modified SBS and $E_b = 16.0 \text{ V } \mu\text{m}^{-1}$ for carboxylic acid modified SBS.^[24, 94] This indicates the reduction in breakdown strength is linked to the general size of the grafted dipole rather than the differences in the functionality of the dipoles used.

A different approach for using thiol-ene click chemistry has been to synthesise siloxane chains from cyclic monomers containing vinyl groups to provide double bond functionality in the elastomer after a ring opening polymerisation. [73, 82] For example, chloropropane-thiol (TC3a) and 3-mercaptopropionitrile (TC3b) were grafted to PVMS-g-PDMS. This work demonstrated that the main influence on the relative permittivity when grafting organic dipoles to an elastomer is the dipole moment magnitude. However, it was also determined that other factors such as the water sorption ability of the organic molecule had secondary influences on the dielectric properties, leading to unexpected results; see section 4.1 for further information. [82]

100 mol% of 3-mercaptopropionitrile was grafted to PVMS. 3-mercaptopropionitrile is an analogous molecule to allyl cyanide. The grafting led to similar increases in the relative permittivity for both the uncrosslinked (TC4) and crosslinked elastomer (TC5), ε_r = 18.4 and ε_r = 17.4 respectively, in agreement with previous studies in which crosslinking had no direct impact on the dielectric properties.^[84] These increases are similar to grafting 89 mol% of allyl cyanide where a permittivity of ε_r = 15.9 was reported, indicating that the additional sulphur group does not have any significant impact on the structure of the overall elastomer. Similarly the loss of the elastomers is high and approaches ε' = 1 for the uncrosslinked elastomer (TC4)^[73] and ε' = 5 when crosslinked (TC5).^[98] These high values correlate to the

reported dielectric loss for allyl cyanide of ϵ' = 2.5 and follow the general trend in the literature that as the grafting level of organic dipoles is increased, the dielectric loss increases.

The mechanical properties of the crosslinked elastomer are also poor, perhaps to be expected with such a high grafting level of 3-mercaptopropionitrile. The strength of the elastomer is low, T = 0.4 MPa with a low stiffness of Y = 0.16 MPa. The breakdown strength of the elastomer is also low, $E_b = 15.6$ V μ m⁻¹. [98] Nevertheless, this material had the highest Figure of Merit values for both actuation and generation for this section and provides a promising outlook for use of this material in future works.

Grafting 100 mol% of 2-(methylsulfonyl)-ethanethiol to PVMS has resulted in the highest relative permittivity value reported so far for chemical modification, ε_r = 22.7 at 10⁴ Hz (TC6). The large increase can be attributed to the high dipole moment of the sulfonyl group. This was accompanied by a tan $\delta \sim 0.05$. No mechanical properties were however reported for this system. Promisingly, grafting 80.6 mol% of 2-(methylsulfonyl)-ethanethiol resulted in a permittivity of ε_r = 20.4 and a similar loss as when grafting 100 mol%. [99] This could allow improved mechanical properties for the elastomers with a minimal impact on dielectric properties. The positive result from 2-(methylsulfonyl)-ethanethiol paves the way for the grafting of other sulfonyl groups to dielectric elastomers for enhancement of dielectric properties. It should be mentioned that this reaction does require the use of thiols which can have a strong odour associated with them. [100] This could potentially lead to elastomers formed using this reaction also possessing a strong odour, something not suitable for energy harvesting applications in everyday applications.

Silicone based nanoparticles in the form of polyhedral oligomeric silsesquioxane (POSS) cages with eight vertices were covalently grafted to SBS to act as a reinforcing crosslinking

agent. The chemically grafted nanoparticles affect the properties of the elastomer intrinsically, which is different from the composites systems discussed in Section 3. The cage was formed from eight molecules of (3-mercaptopropyl)trimethoxysilane which gave each vertex thiol functionality for grafting to SBS. The tensile strength of SBS increased from T = 1.9 MPa to T = 23.4 MPa and the elongation at break decreased when 1 wt% of the POSS cage was grafted to the elastomer backbone as a direct result of the crosslinking that was introduced. [101]

To date, POSS cages have been utilised for low dielectric and insulating applications through grafting or by blending to form a composite, $^{[102,\ 103]}$ where the relative permittivity of epoxy resin decreased to as low as $\varepsilon_r=2.60$, $^{[103]}$ but increasing properties such as UV shielding for high performance applications. $^{[104]}$ A POSS cage with thiol functionality on all eight vertices was grafted to poly(benzoxazine) using a thiol-ene click reaction. This resulted in an improvement of the mechanical properties due to the crosslinking, and a reduction in the permittivity. Upon grafting 50 wt% of the POSS cage, the permittivity decreased from $\varepsilon_r=3$ for the neat polymer to $\varepsilon_r=2$. $^{[104]}$

4.3. Copper(I) catalysed alkyne-azide cycloaddition reaction

Copper(I) catalysed alkyne-azide cycloaddition reactions (Azide-click chemistry) have been carried out to chemically modify silicone-based elastomers by a copper(I) catalysed cycloaddition reaction between an azide and alkyne group, forming a 1,4-disubstituted product, see **Figure 16**. Using this reaction, a number of molecules have been grafted to the crosslinker used in PDMS elastomers, including molecules with aromatic rings, fluorinated aromatic systems and ferrocene sandwich systems. However, no dielectric data was recorded for these materials,^[105] despite the possible intrinsic value of grafting these groups on the dielectric properties.

Typical reaction conditions for azide click chemistry involve dissolving the azide modified PDMS (AMS) and alkyne modified organic molecule in a dry solvent with Et₃N as a base and Cul as a catalyst. The reaction is stirred for 17 hours at 40 °C after which the product is obtained as an oil in a quantitative yield. ^[106] This form of click chemistry does take longer to form the modified films compared to thiol-ene click chemistry, as the reaction proceeds *via* a different route - a thermally-induced rather than a UV-induced pathway. However, similar to the thiol-ene click reaction, the reaction does produce a high yield of product with no difficult purification techniques required.

Nitrobenzene was grafted to PDMS-g-AMS at different grafting levels and with different lengths of PDMS spacer chains as part of the elastomer backbone to vary the distance between the nitrobenzene groups (AC1a-d). From **Table 8**, grafting 51 mol% of nitrobenzene to PDMS using 1200 g mol⁻¹ spacer chains increased the relative permittivity to $\varepsilon_r = 5.1$ (AC1a). However, by increasing the nitrobenzene content yet further to 100 mol% grafting (AC1b) the permittivity did not increase any further and the Figure of Merit decreased. This is possibly due to a smaller increase in the density of nitrobenzene groups within the elastomer as a larger PDMS spacer chain is used. By increasing the grafting level there is an increase in tan $\delta = 0.04$ for AC1a to tan $\delta = 0.6$ in AC1b, with no increase in relative permittivity.

Regardless of the grafting ratio, a good breakdown strength of E_b = 69.2 V μm^{-1} and 60.5 V μm^{-1} was reported for AC1a and AC1b respectively, suggesting that these silicone-based elastomers would be resistant to electrically induced failures. However, no mechanical properties are reported to allow the determination of elastomer strength and elasticity. By reducing the PDMS spacer chain length from 1200 g mol⁻¹ to 580 g mol⁻¹ the permittivity increases due to an increase in the density of the organic dipole groups within the chain. At

a 42 mol% grafting level (AC1c), the permittivity is already higher than using 1200 g mol⁻¹ spacer chains with 100 mol% grafting. Further increases in the grafting level led to a relative permittivity of ε_r = 8.5 (AC1d). The tan δ values are slightly higher for the shorter PDMS spacer lengths and increases from tan δ = 0.15 for 42 mol% grafting to tan δ = 0.9 for 100 mol% grafting.

The breakdown strength remains high for this level of grafting, $E_b = 64.1 \text{ V } \mu\text{m}^{-1}$ for AC1c and $E_b = 65.0 \text{ V } \mu\text{m}^{-1}$ for AC1d. In fact, the breakdown strength for all of the modified silicone elastomers are higher than the reference PDMS elastomer, $E_b = 55.4 \text{ V } \mu\text{m}^{-1}$. This is due to the purification steps undertaken in the work once the films are formed to remove the metallic copper impurities, as these can affect the dielectric properties of the films formed. [107]

Systems incorporating nitrobenzene and nitroazobenzene modified crosslinkers using azide click chemistry have been reported. As expected, the increases in relative permittivity is much lower when organic dipoles are grafted to the crosslinker compared to the modification of the main silicone chain, as seen in section 4.1. Both nitrobenzene (AC2) and nitroazobenzene (AC3), a mesogenic type organic dipole (see section 4.4.1 for more information on mesogens) increased the permittivity from $\varepsilon_r = 2.8$ to $\varepsilon_r = 3.1^{[105]}$ and $\varepsilon_r = 3.2^{[108]}$ respectively. Different lengths of PDMS chains were used in this work, however an increased chain length appeared to have no detrimental impact on the permittivity. The dielectric loss for nitrobenzene modified crosslinkers is low, $\varepsilon' = 0.001$, approximately an order of magnitude better compared to a purely azide modified crosslinker in the elastomer. This is a large increase considering only a 0.25 wt% loading of nitrobenzene modified crosslinker was used. [105] For nitroazobenzene modified crosslinkers, the increase in tan $\delta = 6.0 \times 10^{-4}$ to tan $\delta = 5.2 \times 10^{-4}$, a small increase for a larger loading of organic dipole. At this

concentration, the breakdown strength increased from $E_b = 110 \text{ V } \mu\text{m}^{-1}$ to $E_b = 124.2 \text{ V } \mu\text{m}^{-1}$. The nitroazobenzene modified crosslinker increased the breakdown strength of the structure either via intermolecular interactions from the nitro groups or by stabilisation of charge through the aromaticity of the dipole. However, at higher grafting levels of nitroazobenzene, the permittivity remains the same but a decrease in breakdown strength is observed to $E_b = 57 \text{ V } \mu\text{m}^{-1}$ at a 3.6 wt% loading. This shows that at 1.35 wt%, the threshold at which the organic dipole has a negative effect on the breakdown strength has yet to be reached. $^{[109]}$

4.4. Grafting of mesogens

When electrostrictive graft elastomers consist of crystallisable side chains attached to the main chains, the grafts on the backbone can crystallize to form physical cross-linking sites to form three-dimensional elastomer network and generate electric field responsive polar crystal domains. These polar crystal domains provide an opportunity to contribute to electromechanical functionality. When an electric field is applied to the elastomer, the polar domains rotate to align in the field direction due to the driving force generated by the interaction between the net dipoles and the applied electric field. The rotation of grafting side chains induces the reorientation of backbone chains, leading to a deformational change. When the electric field is removed, the polar domains randomize leading to dimensional recovery. [110]

Of particular interest are mesogens, which are small, 'rod-like' organic molecules,^[111] typically two nanometres long and half a nanometre thick^[112] that create a crystal phase in a liquid crystal elastomer (LCE), known as a liquid-crystalline monodomain.^[113] Examples of mesogens are shown in **Figure 17** with azo groups,^[114] ferrocenyl groups^[115] and aniline groups.^[116] More specifically, the order of alignment of the mesogens within the LCE

influences the properties exhibited by these crystalline monodomains. There are four orientations in which the monodomains can exist, which will now be described.

Firstly there is the isotropic phase, in which there are no long-ranged positional or orientational orders exhibited by the mesogens.^[111] This type of ordering is found in LCE at higher temperatures where the kinetic energy of the mesogens is such that it can overcome any intermolecular interactions.^[111] On the other extreme, there is the crystalline phase in which long-range positional and orientational order are observed, typically for LCE at lower temperatures. In the crystalline phase, the mesogens will have regular lattice sites and will be aligned in a common direction^[111] making them anisotropic.^[117]

The two intermediate phases, referred to as mesophases, are the nematic and smectic phase. The nematic phase does not exhibit any long-range positional order, however the majority of mesogens have a common directionality in their orientation. [111] Typically, most LCE exist between the isotropic and nematic phase. [118] The smectic phase is where the mesogens have formed regular layers which can slide over each other easily but also have a common directionality. [111]

The mesogens can be incorporated within the polymer backbone as a block copolymer or as side chain groups in one of four ways. The first method involves a competitive reaction between the crosslinker of the elastomer and the mesogens units to become side chain groups^[117] through a catalysed reaction between vinyl groups and typically Si-H bonds, making this approach very desirable for the modification of polysiloxanes.^[119] However, the drawback of using this 'one-pot' synthetic method is the resulting elastomers are typically difficult to purify.^[111, 120]

The second synthetic route involves an already modified chain which is crosslinked using multifunctional crosslinkers to generate the elastomeric network.^[117] This allows the

modified individual polymer chains to be purified and form low molecular weight by-products prior to crosslinking. [120]

The third method of incorporating mesogens is to chemically modify the polymer so that the mesogens and crosslinkable groups are already attached to the backbone^[117] followed by the application of UV light, resulting in crosslinking.^[121]

The fourth method uses modified monomeric units with mesogens in which the polymer is then synthesised and crosslinked via radical polymerisation through vinyl end groups on the monomers. [117] For example, Lub *et al.* used UV light to carry out the polymerisation and crosslinking simultaneously. [122]

In LCE, the orientation of mesogen units can be manipulated during synthesis to induce a stronger common directionality^[111] or to change the direction of their alignment.^[123] Firstly, the application of an electric field to the LCE causes the mesogens to align parallel to the electric field followed by crosslinking of the elastomeric chains to lock the mesogens into place.^[124] An alternative method of manipulation is to apply a magnetic field to align mesogens orthogonally to it,^[125] or to chemically treat the surface. The orientation of the mesogens can then be locked into place by crosslinking of the elastomeric chains.^[118] The advantage of this approach is that the LCE can exhibit a much stronger dielectric response, as the polarity of the LCE is enhanced.

The LCEs can respond rapidly (10 ms)^[126] at low electric fields (1.5 $^{\sim}$ 25 MV·m⁻¹) compared to other field activated electroactive polymers, but they are limited by the low actuation strain ($^{\sim}$ 10%) and low energy density^[14]. In comparison, dielectric elastomers such as acrylic and silicon elastomers exhibit larger stains (10 $^{\sim}$ 400%) and higher energy densities (3 $^{\sim}$ 8 MJ·m³), but require high electric field (100 V· μ m⁻¹) to activate.^[12] The LCEs with cholesteric

liquid crystals exhibited actuation strains up to 30%, modification of LCEs can be achieved through the following methods.

4.4.1. Atom transfer radical polymerisation (ATRP)

ATRP is a versatile copper mediated living radical polymerisation technique^[127] used for the polymerisation of highly controlled block copolymers resulting in a low polydispersity Index (PDI) for the product, with the PDI tending to 1.^[128] The reaction proceeds via the activation of a radical initiator, in which a carbon-halide bond is broken to generate a free radical. This free radical reacts with vinyl groups on the monomer units to propagate the reaction, forming a polymer, see **Figure 18**.^[127]

Typical reaction conditions for ATRP involve a reaction under nitrogen between the monomer, CuBr, 1,1,4,7,10,10-hexamethyltriethylenetetramine, anisole and methyl-2-bromo-2-methylpropionate at 90 °C for 10 hours. Purification steps for this reaction involve using an alumina column to remove the copper catalyst, followed by precipitation to obtain the purified polymer. [123]

This reaction has been used to incorporate rod-like mesogen groups as side chains or as part of the elastomer backbone. LCE were first hypothesised as exhibiting actuation properties in 1975^[129] and first experimentally proven in 1997.^[130]

Most studies have focused on the actuation of the LCE upon a thermal^[131, 132] or photo stimulus^[132, 133] when incorporating mesogens as side chain groups. However, some dielectric studies have been carried out with respect to LCE by forming a block copolymer between the mesogens and PDMS or poly(n-butyl acrylate) (PBA), see **Table 9**.

An example synthesis from Madsen *et al.* for the formation of monomeric 11-(4-cyano-4'-biphenyloxy)undecyl methacrylate (11CBMA) is achieved via a multistep reaction where 4'-cyano-4-hydroxybiphenyl, K_2CO_3 and KI are heated under reflux in dry acetone for 30

minutes. 11-bromo-1-undecanol is added and refluxed for a further 12 hours before removal of the solvent and purification by recrystallization to obtain pure 11-[(4-cyano-4'-biphenylyl)oxy]undecanol. This product is then dissolved with N,N'-dicyclohexylcarboiimide and 4-dimethylaminopyridine in dry dichloromethane (DCM) and stirred for 30 minutes. A solution of methacrylic acid dissolved in DCM is added dropwise before further stirring of the reaction mixture for 17 hours. The precipitate is removed and solvent evaporated, and the remains are purified using flash chromatography with silica gel to obtain pure 11CBMA, see **Figure 19**.^[123]

Synthesis of 11CBMA results in a high overall product yield, 89.1%. The formation of the PDMS-g-P11CBMA_n diblock copolymer LCE also results in a high yield of 81.1%. PDMS diblock copolymers containing 40 units of 11CBMA to form PDMS-g-P11CBMA₄₀ (AT1a) increased the relative permittivity to ε_r = 6.42, compared to ε_r = 2.38 from PDMS. The loss tangent also remained low at tan δ = 0.024. The alignment of the mesogens was identified using Polarised Optical Microscopy (POM), which revealed that before formation of a diblock copolymer, the mesogens were aligned in a smectic-A fashion. However when the PDMS-g-P11CBMA₄₀ diblock copolymers were formed, POM revealed that the phase structure of mesogens became undefined. [123]

The literature has shown the alignment of mesogens can be modified upon application of an electric or magnetic field, or by chemical treatment of the LCE. [124, 125] Mesogens were homogeneously aligned within the LCE, so that their orientation is parallel to the film surface (AT1b). This was achieved by rubbing the surface of the LCE in a single direction, with the homogeneous alignment verified by POM. However, the smectic-A phase structure was still lost. This alignment led to a decrease in the permittivity from $\varepsilon_r = 6.43$ to $\varepsilon_r = 5.37$,

since in this orientation the mesogens have a lower dipole polarisability whilst maintaining a similar tan δ . [123]

Modification of the alignment of mesogens so that they are homeotropically aligned (perpendicular to the surface of the film) by chemical treatment of the LCE (AT1c) increased the relative permittivity from ε_r = 6.43 to ε_r = 7.29 with a similar tan δ = 0.024. The LCE also had an undefined phase structure suggesting that when the mesogens are part of the diblock copolymer, microdomain structures are more difficult to form. As the relative permittivity was dependent on the orientation of the mesogens within the LCE, and maintained a constant tan δ , it demonstrated that the orientation of the mesogens within an energy-harvesting device would be possible. Neither the mechanical properties nor breakdown strength have been reported for these LCEs.

11CBMA has also been used to form a triblock copolymer LCE with PBA in the form of P11CBMA_n-g-PBA-g-P11CBMA_n. Once again, the mesogens had a smectic microphase structure that disappeared upon formation of the triblock copolymer, indicating that formation of the copolymer disrupts the microphase structure of the product. For the LCE P11CBMA₅₃-g-PBA-g-P11CBMA₅₃ the maximum permittivity was ε_r = 7.82 when the film was thermally annealed, with a low tan δ = 0.032 (AT2a). Thermal annealing of the elastomers provides a uniformity in the direction of alignment for the mesogens, resulting in a high permittivity. [134]

This impact of annealing on the dielectric properties was explored on the triblock copolymer by investigating the effect of thermal annealing (AT2b), solvent annealing (AT2c) and no annealing (AT2d) on P11CBMA₄₀-g-PBA-g-P11CBMA₄₀ films. No annealing resulted in the lowest relative permittivity of ε_r = 4.19, as the alignment of mesogens is the least ordered and produced the lowest dipole moment. [134] Solvent annealing in xylene produced the best

dielectric properties for the solvents investigated with an increased permittivity of ε_r = 5.50 (AT2c), showing that the slow evaporation rate of xylene and the effect on the nanophase structure of the elastomer, resulted in an increased polarisability from an increased order of mesogen alignment.

Thermal annealing of the elastomer film resulted in the highest relative permittivity, ε_r = 6.56 (AT2b). This demonstrated that thermal annealing was the most successful for creating a uniform alignment of mesogens. However, the rate of heating and cooling was only described as "controlled," with no physical rates given. If the thermal annealing been conducted at a slower rate, an even higher order of alignment for the mesogens could have been obtained, increasing the polarisability and permittivity further. Therefore, the method of annealing and the conditions under which annealing takes place when using LCE should be considered for optimisation of the dielectric properties.

4.4.2. Alternative reactions

Mesogens have also been grafted to elastomers using other reactions, see **Table 10**. 2,2'-[[4-[(4-nitrophenyl)azo]phenyl]imino]bisethanol (DR19) was covalently grafted to PDMS in a condensation cure reaction, as in **Figure 20**. [137] Grafting 13.2 wt% of DR19 increased the permittivity from ε_r = 2.72 to ε_r = 4.88 (OR1b). The relative permittivity is lower than when highly polar DR1 was grafted to PDMS at a lower grafting level (see section 4.1), even though the core structure and polarity of the molecules are similar. This indicates there are other factors influencing the relative permittivity, such as water sorption [82] and steric hindrance vs chain interactions affecting the free volume available within the elastomer. [137] There are large differences in the mechanical and electrical properties when DR19 is grafted at a 10.3 wt% (OR1a) and at 13.2 wt% (OR1b). At 10.3 wt% grafting, the elastomer exhibits a T=1.15 MPa, Y=0.37 MPa and $\lambda_{max}=525\%$. Once the grafting increases to 13.2 wt%, the

strength of the elastomer decreases to T=0.90 MPa, with a increase in Y=0.73 MPa and $\lambda_{max}=225\%$. There is also a decrease in the breakdown strength by increasing the grafting level, from $E_b=89.4$ V μm^{-1} at 10.3 wt% to $E_b=56.7$ V μm^{-1} at 13.2 wt%^[137] as the higher grafting level of polar moieties increases the probability of short term breakdown of the structure.^[109] This results in higher Figure of Merit values for both actuation and generation for grafting 10.3 wt% of DR19 compared to 13.2 wt%. Overall, the electrical and mechanical properties are suitable for energy harvesting when there is a slightly lower grafting of DR19. Given the difference in the relative permittivity between grafting DR19 and grafting DR1 in section 4.1, it would be of interest to compare the difference in mechanical and electrical properties of these elastomers to determine which organic dipole would be most suitable for energy harvesting applications.

A different approach to chemical grafting is to graft polymeric chains with favourable properties directly to the native elastomer, to reduce phase separation between different polymers due to incompatibilities between their structures. [138] It also allows for organometallic structures to be covalently attached between the two polymer chains to increase the dielectric properties, whilst at the same time preventing agglomeration of metal nanoparticles within the elastomer which reduces the breakdown strength. [139]

Examples of this approach involve grafting conductive PANI to maleic anhydride (MA), which is already attached to SEBS, through ring opening reactions (OR2a and OR2b). [139] Other work has grafted PANI onto polyurethane (PU) through a copper phthalocyanine (CuPc) macrocyclic ring (OR3a and OR3b). [138] Both incorporated PANI due to its ability to increase the dielectric constant through the percolative phenomenon, where a sharp rise in conductivity is observed for nanocomposites by the formation of PANI nanodomains in the

elastomer structure.^[140] The addition of CuPc additionally increases the permittivity of the native elastomer.

For OR2a, the grafting of 2 vol% PANI resulted in an increased permittivity from ε_r = 2 to ε_r = 5.5 at 10^4 Hz. However, if the grafting level was increased further to 2.1 vol%, the relative permittivity increased to ε_r = 10 due to incomplete grafting of PANI resulting in a free polymer within the SEBS elastomer. This causes the PANI chains to interact with each other through the percolative phenomenon, increasing the permittivity and the conductivity of the elastomer. This effect is also seen in the difference in tan δ from grafting PANI, where the increase of 0.1 vol% to 2.1 vol% of PANI results in an increase from tan δ = 0.10 to tan δ = 0.40. [139]

The mechanical properties and breakdown strength of the elastomer before reaching the percolation threshold was a strength of T=5 MPa, Y=1.6 MPa and $\lambda_{max}=650\%$. The breakdown strength of the elastomer remains high compared to the unmodified SEBS-g-MA elastomer at $E_b=110$ V μm^{-1} . However, when the grafting level was increased to 2.1 vol% PANI, the breakdown strength decreases significantly to $E_b=65$ V μm^{-1} due to the percolation threshold being reached. No mechanical properties were reported at this grafting level.

Other work on OR3x grafted CuPc and PANI to PU chains. CuPc is a macrocyclic molecule, commonly used in dyes, which can display a good conductivity when polymerised. [141] Grafting 23 vol% of CuPc molecules to PU increases the relative permittivity from ε_r = 9 to ε_r = 30 (OR3a) and only increases the dielectric loss marginally, from ε' = 0.05 to ε' = 0.15. However, by grafting these macrocyclic molecules to the elastomer, the flexibility of the elastomer drops significantly, with an increase in the Young's modulus from Y = 20 MPa to Y = 60 MPa as a direct effect of the addition of the macrocyclic rings. [138]

PANI was grafted to the modified system in OR3a to form an elastomer of PU-g-CuPc-g-PANI (OR3b), see **Figure 21**. When 14.4 vol% of PANI was grafted, the relative permittivity increased from ε_r = 30 to ε_r = 105. At the same time, the increase in the dielectric loss only increased to ε' = 0.28, a small increase for such a large gain in permittivity. However, the flexibility of the elastomer decreased further with Y = 90 MPa, $^{[138]}$ making the elastomer too rigid for energy harvesting applications.

A different concept for modifying polymers with conductive aniline was to modify the ends of polystyrene with oligoaniline units, as in **Figure 22**, using azide click chemistry; see section 4.3 for more information. By surrounding the oligoaniline with an insulating polymer, the formation of conductive nanodomains in the structure was encouraged. The presence of the nanodomains increases the interfacial area for polarisable nanodipoles to form, enhancing the overall polarisability of the polymer. End capping using aniline also prevents large scale agglomeration of the groups, reducing the dielectric loss of the polymer. From this, the relative permittivity increased from $\varepsilon_r = 2.7$ for polystyrene to $\varepsilon_r = 3.6$ when 7.94 wt% oligoaniline was grafted with a low loss maintained, $\tan \delta = 0.01$ (OR4a), due to the lack of conductive pathways forming.

The polystyrene was doped with camphorsulfonic acid (CSA), a large bulky acid, to enhance the relative permittivity of the system (OR4b). In DFT studies, bulky organic acids have been shown to increase the electronic properties of aniline containing polymers. [143] Furthermore, CSA is able to interact with the nitrogen in oligoaniline, [144] stabilising the dopant in the polymer. It is hypothesised that the acid enables a greater electron transfer between the acid and the aniline, enhancing the conductivity between the two. Small Angle X-Ray Scattering data of the system showed that the ordered oligoaniline nanodomains were not formed when CSA was added, instead observing disordered domains with large interfacial

regions between aniline and polystyrene. The electrical properties of the polystyrene near to the large interfaces could be enhanced by this approach, increasing the polarisability of the polymer throughout the structure. This was correlated by the increase observed in the permittivity, where enhancement from $\varepsilon_r = 3.6$ to $\varepsilon_r = 22.6$ was reported when a combined amount of 10.9 wt% of oligoaniline and CSA was added. In addition, the loss tangent for the system was only tan $\delta = 0.02$. [142]

This methodology of end capping could be applied to other elastomers such as SBS or SEBS with relative ease. A viable modification approach could be further supplemented by grafting of dipoles into the butadiene segment of the structure. This type of structure, in which multiple segments in a block copolymer are modified, has yet to be reported in the literature.

5. Flexible elastomeric energy actuators and generators

The need for chemical modification of dielectric elastomers is ultimately for their use in real world applications. The desired improvements in electrical properties and mechanical properties enable dielectric elastomers to actuate at greater strains with lower applied voltages. Likewise, it also enables the elastomers to harvest greater amounts of energy from more easily deformable elastomers which have a greater capacitance to store energy during an energy harvesting cycle.

This section discusses the use of dielectric elastomers as actuators and in energy harvesting devices, including the use of cyanopropyl modified dielectric elastomer in an energy harvesting set-up. The emphasis here is on how the chemistry of the materials have improved device performance rather than device design, which has been covered in other excellent reviews.^[14, 39, 145]

5.1 Dielectric elastomers as electromechanical actuator (DEA)

The widely used commercial dielectric elastomers are silicone rubbers, such as Dow Corning HS3 Silicone and Nusil CF 19-2186 Silicone; 3M acrylic elastomers such as VHB 4910 due to their relatively high permittivity and high breakdown strength; polyurethanes, and other thermoplastic elastomers, such as SBS and SEBS.

Dielectric elastomer actuators (DEAs) are a form of electromechanical transducer, made with an incompressible and highly deformable dielectric medium. Under an electric field across the parallel plates of a capacitor, the columbic forces between the charges generate a stress, i.e., the Maxwell stress, causing the electrodes to move closer. As a result, the elastomer is compressed in thickness and expanded in the lateral direction. Therefore the electric field that can be applied to the dielectric elastomer, the dielectric response of the elastomer and the ease in which the elastomer can be deformed are all key properties for producing a material with superior actuation abilities. Hence, the Figure of Merit for actuation shown in section 1 takes into account these three factors.

The actuation strain is expressed as **Equation 7**,

$$S = \frac{P}{V} = \frac{\varepsilon_0 \varepsilon_r E^2}{V} = \frac{\varepsilon_0 \varepsilon_r}{V} (\frac{V}{d})^2 \tag{7}$$

where S is the thickness strain induced by the applied electric field, P is the effective

compressive stress induced by the applied electric field, ε_r is the relative permittivity of the elastomer, ε_0 is the permittivity of free space (8.85 × 10^{-12} F/m), E is the applied electric field, Y is the modulus of elasticity, V is the voltage and d is the thickness of the sample. [23] Equation 7 indicates that the actuation performance of dielectric materials for a given applied voltage can be increased by either increasing ε_r , reducing Y of the material or using films with low thicknesses. The ratio of ε_r/Y is often used to express the electromechanical sensitivity of a material since it is proportional to the change in capacitance for an applied stress and S is proportional to this material index for a specific applied electric field.

This working principal has been used to develop dielectric elastomer devices for unique applications. Research involves developing elastomers and the set up behind the actuators in order the make them more efficient at lower voltages and have faster response times, such as for the development of artificial muscles. [147] One recent example is PDMS used in actuation mode to act as a gripping device by using carbon filled polyurethane shape memory polymer electrodes. Before application of an voltage, the polyurethane was rigid. This provided the force for gripping objects with no applied electric field. Upon application of 300 V, joule heating reduces the modulus of the polyurethane electrodes by 200 times and allowed the PDMS to actuate and release any object it was holding. [146] PDMS was chosen due to its relatively high actuation figure of merit, see Table 1, primarily due to its low modulus of elasticity, which arises from a relatively low degree of crosslinking, between the polymer chains.

Another example is to create a microfluidic pump using the actuation mode of the elastomer. As can be seen from **Figure 23**, the elongation of the VHB 4910 with carbon black electrodes under an applied voltage was utilised to form a pumping action by attaching it to a pull-up spring. The spring provided the tensile force to pull the elastomer in an upwards direction. A maximum flow rate obtained was 40 µl·s⁻¹ at a frequency of 4 Hz under a 4.2 kV voltage. The VHB 4910 elastomer offers a large strain and actuation performance due to its combination of branched aliphatic groups and lightly crosslinked network structure. [148]

For actuation devices, the shape and design for the device influences the direction and efficiency in which the material can actuate under an applied field. [39, 146, 148] The material selected for actuation influences the magnitude of actuation for a given applied voltage. Chemically modified dielectric elastomers typically exhibit higher relative permittivity's and lower Young's modulus' and so may prove crucial for the development of devices which can

actuate at greater strains under reduced electric fields. Several examples shown in section 4 have exhibited Figure of Merit values for actuation greater than 1, suggesting that these materials are more effective for in actuation devices than PVDF. Future research should incorporate these modified elastomers in devices to understand whether the theoretical superiority of these materials translates successfully into practical applications.

One example on soft robots involves the use of a silicone elastomer to develop a 'soft gripper' with highly compliant soft electrodes. This actuated under an applied voltage of 3.5 kV with the claws coming together to tighten around objects where the authors were able to demonstrate their device picking up objects of over 80 g including oil cans, Teflon tubes, thin membraned water balloons and an uncooked chicken egg,^[149] see **Figure 24**. This actuation mechanism is in contrast to the previous soft gripper example made from VHB 4910, as the application of zero voltage is the release mechanism in this case.

Other innovative robots include the development of an autonomous fish capable of swimming in three dimensions and diving using a silicone elastomer. The autonomous robotic fish was powered by a battery and received commands using a built-in wireless assembly. Impressively, the authors were able to demonstrate the ability of the fish to swim entire lengths of a 13.25 m pool for 40 minutes, covering approximately 130 m in total. ^[150] In addition, soft robots that are able to mimic animalistic movements such as crawling have been developed using silicone rubber consisting of chambers that inflate upon actuation to induce movement. As a maximum, the soft robot was able to cover 92 m in one hour. ^[151] For a detailed account of the current state of actuating soft robots and their set-ups and designs, please see the following excellent reviews. ^[16, 152, 153]

5.2. Dielectric elastomers as electromechanical generator (DEG)

Whilst in generator mode, the external mechanical energy used to deform the dielectric elastomer generates and leads to the storage of elastic energy, which is then harvested. The working mechanism of dielectric elastomer harvesters is shown in Figure 1B.

Enhancement of the physical properties of dielectric elastomers can maximise the mechanical energy that can be converted and maximise the amount of deformation and change in capacitance that can be achieved. Increasing the elastomer extensibility is therefore key for maximising the elastic energy stored in the material and providing a larger change in area and thickness to enable a large change in capacitance. Ensuring a high E_b allows the dielectric elastomer to be placed under a higher electric field, increasing the charge density at the surfaces of the elastomer. This means that more energy can be harvested when the dielectric elastomer unloads, bringing more charge closer together and thus increasing the energy output. Thus the Figure of Merit for generation is a combination of relative permittivity and the breakdown strength of the material, to demonstrate how the modification alters the overall ability to convert mechanical energy to electrical energy.

A dielectric elastomer harvesting device can be operated in three different ways: (1) under constant charge; (2) under constant voltage and (3) under constant electric field. From this, **Equation 8** and **9** describe the maximum amount of energy that can be harvested from the devices: [154]

$$u_Q = u_V = \frac{1}{2} \cdot \varepsilon_r \cdot V \cdot E_{max}^2 \left[1 - \frac{A_{min}^2}{A_{max}^2} \right]$$
 (8)

$$u_E = \frac{1}{2} \cdot \varepsilon_r \cdot V \cdot E_{max}^2 \cdot 2 \ln \left[\frac{A_{max}}{A_{min}} \right]$$
 (9)

where ε_r is the dielectric constant, V is the volume, E_{max} is the maximum electric field the dielectric elastomer is subjected to and A is the change in area of the elastomer. [154]

To harvest the greatest amount of energy, the dielectric elastomer needs high driving voltage (500V ~10 kV)^[3], which is restricted by the breakdown strength of the elastomer. The use of self-priming circuits could present an ideal alternative overcome this issue.

Self-priming circuits work by retaining part of the charge harvested from the previous cycle to build the electric field in which the dielectric elastomer is placed for the next cycle. This acts as a voltage booster, which can build on the field applied to the elastomer, thus allowing a much lower and more desirable initial voltage to be applied. The working mechanism for devices using self-priming circuits is similar to that of the previous mechanism. After deformation and charging of the dielectric elastomer has been applied, the dielectric elastomer is unloaded. Some of the charge is transferred into the self-priming circuit to be stored. When the elastomer undergoes the next deformation, the voltage within drops until the threshold for charge transfer from the self-priming circuit is reached

The design and set-up used for creating an energy harvesting device has shown to be influential in the energy generation and efficiency. Early devices used high voltages from external sources, typically created from high voltage transformers. [5, 156, 157] This increased the weight of the system, the complexity for designing the device and the overall cost of producing the device. [157, 158]

(Figure 25).[155]

McKay *et al.* developed a dielectric elastomer energy generator using VHB 4905 attached to a frame with two pairs of dielectric elastomer generators using a self-priming circuit set-up, thus not requiring high voltages to be externally applied. Two pairs of elastomers were attached to a frame and pre-stretched to nine times their original size that were coated with carbon grease electrodes. The set-up ensured that the two pairs of generators were 180° out of phase with one another so that when one pair was stretched, the other was in a

relaxed state.^[158] This enabled charge to flow from one pair of elastomers to the other through diodes to act as the mechanism for boosting the voltage.^[158] An initial voltage of 10V was stored in the dielectric elastomer using an external capacitor power bank, utilising the capacitance of the elastomer.

The set-up consisted of only six diodes for external circuitry and enabled the voltage in the device to be boosted from 10 V to 2 kV in 4.7 seconds at a rate of 3 Hz. [158] An energy output of 4.4 mJ per stroke with an efficiency of 7.8% was achieved from this device, which corresponded to an energy density of 12.6 mJ g⁻¹ for the material. The weight of the external circuitry was just 1.26 g and could be implemented in much larger devices as the diodes used were suitable for forward currents 1000 times higher than used in the small device. [158]

This set-up was further improved to require no external circuitry. ^[159] The diodes were replaced with dielectric elastomer switches, which were comprised of piezoresistive electrodes (**Figure 26**). These were used to connect the pairs of dielectric elastomers to control the flow of charge upon the changes in stretch of the material. The piezoresistive electrode had a resistance of the order of $M\Omega$ when in a relaxed state which increased to $G\Omega$ in the stretched state. ^[159] As a result, the energy density of the material increased to 10 mJ g⁻¹ with an efficiency of 12% at 3 Hz and the device was able to boost itself from 10 V to 2 kV in 11.5 seconds. ^[159]

However, these energies are far below that of the maximum theoretical energy density of the material of 6.3 J·g⁻¹ for an idealised dielectric elastomer, calculated by Koh *et al.*^[160] Suggested ideas for improving the experimentally obtained energy density are using higher electrical fields, higher frequency deformation, improving the dielectric elastomer generator design further and improving the electrical load matching. ^[157, 158] Clearly there is potential

for improving material properties and device performance by the chemical modification processes outlined in this review.

The dielectric elastomer selected for an energy generator should be carefully considered. In these energy generators, VHB 4905 is used. From Table 1, the Figure of Merit for generation for VHB 4905 is 0.052, relatively high to the value obtained for dielectric elastomers. However, VHB 4905 is a viscous material and the high viscous losses result in a reduction in efficiency of the device, as charge leaks through the membrane. [161] It has been suggested that development into dielectric elastomer switches could reduce the losses that they exhibit which would in turn reduce the initial voltage required to prime the self-priming circuit. The aim is so that ambient radiation would be able to supply the initial priming charges. [159] Alternatively, the use of a piezoelectric polymer in the energy generator could also be employed. [159]

Using a thin film of dielectric elastomer in a generator device enables the breakdown strength of the material to be as high as possible. It was found that the most efficient configuration for energy harvesting devices are laminate multi-layered films as they promote the advantageous polarisations in the materials to the greatest degree. [7] Innovative applications such as harvesting energy from wind and wave power as well as manual mechanical impulses have been investigated. In short, wind energy was harvested by the rotation of a turbine attached to a moving rod to deform the elastomer whilst wave energy used air in a chamber to deform the elastomer to a different extent based on the oscillation of the wave. [162, 163] The mechanical properties, high breakdown strength and low cost of fabricating dielectric elastomer devices makes their use in both small- and large-scale applications feasible, with the focus applied on increasing the dielectric properties of these materials.

The small-scale application of dropping objects on a supported dielectric elastomer in a circuit could be extended to harvesting energy from larger scale applications such as turning door handles or simply walking along a floor in a corridor. The set-up used contained cyanopropyl modified PHMS films modified with up to 12.5 wt% of cyano groups which were placed between gold-plated copper electrodes and connected in a circuit to an oscilloscope. The modification of PHMS resulted in an elastomer that had an increased permittivity and reduced tensile strength compared to the unmodified silicone elastomer. Using this elastomer, metal balls of different weights, 12.7 g and 8.7 g, were dropped onto the elastomer and the harvested energy was recorded.

The outcome indicated that the energy harvested was dependant on several factors. In this set-up, the weight of the ball was linked to the energy harvested, as a heavier ball lead to a larger deformation of the elastomer. The optimum system for harvesting mechanical energy using the small metal balls was the elastomer grafted with 3 wt% of cyanopropyl groups, system B, harvesting 460 nJ of energy compared to 151 nJ for system A, which had a grafting level of 12.5 wt% of cyanopropyl groups (Table 11). This was marked improvement on the pure the unmodified silicone elastomer which had a maximum energy output of 94 nJ. The results demonstrated a good correlation between the electromechanical sensitivity of dielectric elastomers and the ability of the system to harvest energy. However, the stiffness of A was higher than B, preventing the deformation of A when small weights are used, thus harvesting less energy. In comparison, a PDMS elastomer containing no cyanopropyl harvested only 93.6 nJ of energy, showing an increase in energy harvesting of over four times for system B. [164] The Figures of Merit for actuation and generation below are normalised to PVDF; in this case for energy generation mode the generation figure of merit is significantly lower than PVDF but since in this case the change in dimensions, and

capacitance, is due to an impact rather than an applied strain, it is beneficial to have a reduced *Y*. As a result, the actuation figure of merit is a more relevant measure of performance since the stiffness is a factor.

Dielectric elastomers have been used as wave energy harvesters to replace concrete and metal structures for use in salt water conditions, which would corrode over time due to prolonged exposure. Dielectric elastomers also represent a low cost, lightweight and low toxicity approach as compared to metal or concrete structures. In this example, a large dielectric wave harvesting device was able to harvest on average 2.8 W under a bias voltage of 1600 V and wave frequency of 0.7 Hz, which represented an energy conversion efficence of 20%. [165]

It is clear that the manufacture of successful actuation and energy harvesting devices depends on both the design of the set-up and the dielectric elastomer used for the device. For energy generator devices, the design of the set-up is important for maximising the practical energy density obtained from the elastomer, ^[159] as well as to enabling the device to be self-priming for a minimal input of energy per harvesting cycle. ^[155] Chemical modification of the elastomers has shown to increase the energy harvested from a micromechanical input device by over four times. ^[164] This device demonstrated the fine balance between the positive increases in the relative permittivity of a dielectric elastomer, against the reduction of the breakdown strength and increase in stiffness of a material with further chemical modification up to 12.5 wt%. However, to date no modified materials have exceeded the Figure of Merit for generation value of 1, that of PVDF. Some recent examples of PVDF energy harvesting devices are given in the following references, ^[166] where these typically demonstrated an ability to harvest energy in µW quantities. This is primarily due to the high breakdown strength of PVDF, which has not yet been matched in chemically

modified dielectric elastomers, although PVDF suffers from a low elastic strains (for harvesting) and relatively high stiffness (for actuation).

Overall, it has been shown that the modification of PDMS has had a positive influence on its energy transducing abilities. This provides a positive outlook that the chemical modification of the different elastomers shown throughout this review and in Table 1 can produce materials with superior actuation and energy harvesting abilities than what is already currently available.

6. Summary and prospective

Dielectric elastomers are materials of significant interest for use in actuators and energy harvesting applications in terms of their tuneable chemical structures, mechanical and electrical properties. ^[21] To enhance their practical applicability, the elastomers need to: (1) have a relative permittivity of at least $\varepsilon_r = 12$, equivalent to that of PVDF, with and low dielectric loss, (2) maintain a high breakdown strength to prevent electrically induced failures of the materials and (3) maintain a balanced tensile strength ($T \sim 2$ MPa), elastic modulus ($Y \sim 1$ MPa) and elongation larger than 200%.

There properties of elastomers can be tuned to some extent by extrinsic approaches, such as blends and composites. However, the chemical modification of dielectric elastomers for energy harvesting is an emerging area due to the ability in intrinsically tuning the structure and electromechanical properties. Covalently bonding of organic dipoles either as side groups or as part of the polymer backbone has been achieved by a range of reactions, including hydrosilylation, thiol-ene click, azide click and ATRP. Hydrosilylation has been commonly used for grafting the vinyl-terminated dipoles to silicone-based polymers allowing a wide range of groups to be grafted whereas thiol-ene click reactions have been carried out on PVMS and SBS elastomers. Azide click chemistry allows the reaction between

an azide modified silicone polymer to be reacted with an alkyne containing polar group. Finally, ATRP allows the incorporation of mesogenic block copolymers to be formed through a free radical polymerisation.

Grafting 2-(methylsulfonyl)-ethanethiol using a thiol-ene click reaction to uncrosslinked PVMS resulted in a large increase in permittivity to ε_r = 22.7. The advantages of thiol-ene click chemistry is that a high product yield can be achieved (up to 100% grafting) in a short time period with minimal purification steps required. However, this reaction does require the use of thiols which can have a strong odour associated with them. This could potentially lead to elastomers formed using this reaction also possessing a strong odour, something not suitable for energy harvesting applications in everyday applications. Some odourless alternatives for odoured thiols have been suggested by Node *et al.* for general use which tend to contain long alkyl chains, but it remains to be seen whether they would be suitable for chemical grafting to dielectric elastomers.

The formation of LCE block copolymers with the mesogen 11CBMA_x have shown good improvements in the relative permittivity with a maximum reported value of ε_r = 7.82 It has been found that the alignment of the mesogen units can significantly affect the polarisability of the LCE and lead to big improvements in the permittivity, without causing increases in the dielectric loss.^[134] The alignment of the mesogens can be influenced by chemically treating the surface or by annealing the elastomer either thermally or using a solvent. Thermal annealing resulted in the highest increase in permittivity for all of the annealing techniques performed due to the most ordered alignment of mesogens formed.^[123, 134]

To date, only chemical modification of siloxane based elastomers and the impact this has on the dielectric properties and mechanical properties has been investigated in any great depth.

This leaves many dielectric materials still to be investigated to determine whether chemical

modification of elastomers can achieve dielectric properties that surpass pure PVDF and approaching modified PVDF systems. It would seem that grafting small, highly polar groups to elastomers would yield the best results for relative permittivity. However, there are usually large increases in dielectric loss, especially when increased water sorption is concerned, and poorer mechanical properties. This raises the question of whether designing organic dipoles to have specific structures could improve the electrical and mechanical properties. Far more work is required to understand which properties of the organic dipoles influence the overall permittivity to design and predict how these would affect the elastomer.

The direct grafting of nanoparticles to the elastomer backbone would also provide improved dispersion of particles within a polymer matrix and enhance the polarity and this has not been explored. Surface modification of fillers such as graphene for attachment could provide useful materials for energy harvesting. Designing polar nanoparticles, such as POSS cages, to attach to polymer backbones would also have the potential to enhance the polarity of a polymer backbone greatly.

In summary, the intrinsic modification of dielectric elastomers by tailoring the polar groups grafted to the polymer backbones will create a 'defect-free' polarisation environment and avoid the electric field inhomogeneity which is otherwise caused by the phase separation and interfacial polarisation in the blends and composites systems.

Improvements to the design of dielectric elastomer generators would increase the harvesting efficiency, and potentially remove the need for external circuitry, in particular high voltage transformers, which represents an important step in increasing the commercial viability of dielectric elastomer generators. However, initial charges are still needed to be stored in the dielectric elastomers before they can be used. Developing materials and

configurations that negate the need for this, and only require environmental radiation to prime the material will be the key for independent dielectric energy harvesting devices to be produced. [159]

Acknowledgements

C.R.Bowen would like to acknowledge funding from the European Research Council under the European Union's Seventh Framework Programme (FP/2007-2013) / ERC Grant Agreement no. 320963 on Novel Energy Materials, Engineering Science and Integrated Systems (NEMESIS).

References

- [1] R. D. Kornbluh, R. Pelrine, Q. Pei, R. Heydt, S. Stanford, S. Oh, J. Eckerle,
- "Electroelastomers: applications of dielectric elastomer transducers for actuation, generation, and smart structures", presented at SPIE's 9th Annual International Symposium on Smart Structures and Materials, 2002.
- [2] D. M. Opris, Adv. Mater., 1703678.
- [3] F. B. Madsen, A. E. Daugaard, S. Hvilsted, A. L. Skov, Macromol. Rapid Commun. 2016, 37, 378.
- [4] R. Kornbluh, R. Pelrine, H. Prahlad, A. Wong-Foy, B. McCoy, S. Kim, J. Eckerle, T. Low, MRS Bull. 2012, 37, 246.
- [5] R. Pelrine, R. Kornbluh, J. Eckerle, P. Jeuck, S. J. Oh, Q. B. Pei, S. Stanford, in *Smart Structures and Materials 2001 Conference*, Vol. 4329, Spie-Int Soc Optical Engineering, Newport Beach, Ca 2001, 148.
- [6] X. Zhang, Y. Shen, Q. Zhang, L. Gu, Y. Hu, J. Du, Y. Lin, C.-W. Nan, Adv. Mater. 2015,27, 819.
- [7] E. Baer, L. Zhu, Macromolecules 2017, 50, 2239.
- [8] C. Wan, C. R. Bowen, J. Mater. Chem. A 2017, 5, 3091.
- [9] T. Soulestin, V. Ladmiral, F. D. Dos Santos, B. Améduri, Prog. Polym. Sci. 2017, 72, 16.

- [10] Prateek, V. K. Thakur, R. K. Gupta, Chem. Rev. 2016, 116, 4260.
- [11] P. Brochu, Q. Pei, Macromol. Rapid Commun. 2010, 31, 10.
- [12] L. J. Romasanta, M. A. Lopez-Manchado, R. Verdejo, Prog. Polym. Sci. 2015, 51, 188.
- [13] J. Biggs, K. Danielmeier, J. Hitzbleck, J. Krause, T. Kridl, S. Nowak, E. Orselli, X. Quan, D. Schapeler, W. Sutherland, J. Wagner, Angew. Chem. Int. Ed. 2013, 52, 9409.
- [14] D. Chen, Q. Pei, Chem. Rev. 2017, 117, 11239.
- [15] Z. Zhenghong, S. Changgeng, G. Yan, R. Emiliano, X. Yuan, Journal of Physics: Conference Series 2016, 744, 012162.
- [16] C. Laschi, B. Mazzolai, M. Cianchetti, Science Robotics 2016, 1.
- [17] Z. Yao, Z. Song, H. Hao, Z. Yu, M. Cao, S. Zhang, M. T. Lanagan, H. Liu, Adv. Mater.2017, 29, 1601727.
- [18] Z.-M. Dang, M.-S. Zheng, J.-W. Zha, Small 2016, 12, 1688.
- [19] J. I. Roscow, C. R. Bowen, D. P. Almond, ACS Energy Letters 2017, 2, 2264.
- [20] R. Pelrine, R. Kornbluh, in *Dielectric Elastomers as Electromechanical Transducers*, Elsevier, Amsterdam 2008, 3.
- [21] J. Zhou, L. Jiang, R. E. Khayat, Soft Matter 2015, 11, 2983.
- [22] J. Lee, H. Kwon, J. Seo, S. Shin, J. H. Koo, C. Pang, S. Son, J. H. Kim, Y. H. Jang, D. E. Kim, T. Lee, Adv. Mater. 2015, 27, 2433; M. Amjadi, A. Pichitpajongkit, S. Lee, S. Ryu, I. Park, ACS Nano 2014, 8, 5154; R. Shankar, T. K. Ghosh, R. J. Spontak, Adv. Mater. 2007, 19, 2218.
- [23] R. Pelrine, R. Kornbluh, Q. Pei, J. Joseph, Science 2000, 287, 836.
- [24] H. Sun, C. Jiang, N. Ning, L. Zhang, M. Tian, S. Yuan, Polym. Chem. 2016, 7, 4072.
- [25] R. M. Grigorescu, F. Ciuprina, P. Ghioca, M. Ghiurea, L. Iancu, B. Spurcaciu, D. M. Panaitescu, J. Phys. Chem. Solids 2016, 89, 97; AzoMaterials, 2001.
- [26] S. S. Banerjee, I. Ramakrishnan, B. K. Satapathy, Polym. Eng. Sci. 2016, 56, 491.

- [27] S. Risse, B. Kussmaul, H. Krüger, G. Kofod, Adv. Funct. Mater. 2012, 22, 3958.
- [28] Advanced Rubber Coatings.
- [29] Goodfellow.
- [30] M. Rabuffi, G. Picci, IEEE Transactions on Plasma Science 2002, 30, 1939.
- [31] T. G. McKay, E. Calius, I. A. Anderson, in *Electroactive Polymer Actuators and Devices* (*EAPAD*), Vol. 7287, San Diego 2009, 72870P.
- [32] B. Chen, M. Kollosche, M. Stewart, J. Busfield, F. Carpi, International Journal of Smart and Nano Materials 2015, 6, 290; V. L. Tagarielli, R. Hildick-Smith, J. E. Huber, International Journal of Solids and Structures 2012, 49, 3409; G. Kofod, P. Sommer-Larsen, R. Kornbluh, R. Pelrine, J. Intell. Mater. Syst. Struct. 2003, 14, 787.
- [33] G. Wu, O. Yano, T. Soen, Polym. J. 1986, 18, 51; Goodfellow, 2017; Matbase, 2017; S. Liu, Z. Cui, P. Fu, M. Liu, Y. Zhang, R. Jia, Q. Zhao, Appl. Phys. Lett. 2014, 104, 172906.
- [34] P. Xu, X. Luo, Y. Zhou, Y. Yang, Y. Ding, Thermochim. Acta 2017, 657, 156; C. Zhou, H. Guo, J. Li, S. Huang, H. Li, Y. Meng, D. Yu, J. de Claville Christiansen, S. Jiang, RSC Adv. 2016, 6, 113762; G. Zhao, B. Huang, J. Zhang, A. Wang, K. Ren, Z. L. Wang, Macromolecular Materials and Engineering 2017, 302, 1600476; N. Matsugasaki, K. Shinyama, S. Fujita, IEEJ Transactions on Electrical and Electronic Engineering 2013, 8, S106.
- [35] A. C. Dent, C. R. Bowen, R. Stevens, M. G. Cain, M. Stewart, J. Eur. Ceram. Soc. 2007,27, 3739; MatWeb-LLC, 2017.
- [36] C. Baur, D. J. Apo, D. Maurya, S. Priya, W. Voit, in *Polymer Composites for Energy Harvesting, Conversion and Storage*, Vol. 1161, American Chemical Society, 2014, 1.
- [37] K. R. Udayakumar, P. J. Schuele, J. Chen, S. B. Krupanidhi, L. E. Cross, J. Appl. Phys. 1995, 77, 3981; MEMSnet; MatWeb-LLC.
- [38] C. Wan, C. R. Bowen, J. Mater. Chem. A 2017, 5, 3091.

- [39] G. Guo-Ying, Z. Jian, Z. Li-Min, Z. Xiangyang, Bioinspiration & Biomimetics 2017, 12, 011003.
- [40] X. Zhang, Y. Shen, Z. Shen, J. Jiang, L. Chen, C.-W. Nan, ACS Appl. Mater. Interfaces 2016, 8, 27236.
- [41] X. Zhou, B. Chu, B. Neese, M. Lin, Q. M. Zhang, IEEE Trans. Dielectr. Electr. Insul. 2007, 14, 1133.
- [42] X. Zhou, X. Zhao, Z. Suo, C. Zou, J. Runt, S. Liu, S. Zhang, Q. M. Zhang, Appl. Phys. Lett. 2009, 94, 162901.
- [43] S. Wu, M. Shao, Q. Burlingame, X. Chen, M. Lin, K. Xiao, Q. M. Zhang, Appl. Phys. Lett. 2013, 102, 013301.
- [44] V. K. Thakur, E. J. Tan, M.-F. Lin, P. S. Lee, Polym. Chem. 2011, 2, 2000.
- [45] V. K. Thakur, E. J. Tan, M.-F. Lin, P. S. Lee, J. Mater. Chem. 2011, 21, 3751.
- [46] R. Li, B. Xue, J. Pei, in *e-Polymers*, Vol. 15, 2015, 439.
- [47] S. J. Laihonen, U. Gafvert, T. Schutte, U. W. Gedde, IEEE Trans. Dielectr. Electr. Insul. 2007, 14, 275.
- [48] A. Hisyam A. Razak, P. Szabo, A. L. Skov, RSC Adv. 2015, 5, 53054.
- [49] H. Bose, D. Uhl, R. Rabindranath, in *Conference on Electroactive Polymer Actuators* and *Devices (EAPAD)*, Vol. 8340, Spie-Int Soc Optical Engineering, San Diego, CA 2012.
- [50] D. Yang, M. Ruan, S. Huang, Y. Wu, S. Li, H. Wang, X. Ao, Y. Liang, W. Guo, L. Zhang, RSC Adv. 2016, 6, 90172.
- [51] D. Yang, F. Ge, M. Tian, N. Ning, L. Zhang, C. Zhao, K. Ito, T. Nishi, H. Wang, Y. Luan, J. Mater. Chem. A 2015, 3, 9468.
- [52] X.-Z. Chen, X. Li, X.-S. Qian, M. Lin, S. Wu, Q.-D. Shen, Q. M. Zhang, Polymer 2013, 54, 5299.

- [53] S. Priya, D. J. Inman, *Energy harvesting technologies*, Vol. 21, Springer, 2009.
- [54] D. Wang, Y. Bao, J.-W. Zha, J. Zhao, Z.-M. Dang, G.-H. Hu, ACS Appl. Mater. Interfaces 2012, 4, 6273; T. Chen, J. Qiu, K. Zhu, X. He, X. Kang, E. l. Dong, Mater. Lett. 2014, 128, 19; W. Tong, Y. Zhang, Q. Zhang, X. Luan, F. Lv, L. Liu, Q. An, Adv. Funct. Mater. 2015, 25, 7029.
- [55] S. Zhao, J. Li, D. Cao, Y. Gao, W. Huang, G. Zhang, R. Sun, C.-P. Wong, J. Mater. Chem.C 2016, 4, 6666; S. Zhao, G. Zhang, Y. Gao, L. Deng, J. Li, R. Sun, C.-P. Wong, ACS Appl. Mater.Interfaces 2014, 6, 22823.
- [56] H. Stoyanov, D. Mc Carthy, M. Kollosche, G. Kofod, Appl. Phys. Lett. 2009, 94, 232905.
- [57] H. Zhao, Y.-J. Xia, Z.-M. Dang, J.-W. Zha, G.-H. Hu, J. Appl. Polym. Sci. 2013, 127, 4440.
- [58] S. Nayak, T. K. Chaki, D. Khastgir, Ind. Eng. Chem. Res. 2014, 53, 14982.
- [59] L. J. Romasanta, M. Hernández, M. A. López-Manchado, R. Verdejo, Nanoscale Res. Lett. 2011, 6, 508.
- [60] D. Yang, M. Ruan, S. Huang, Y. Wu, S. Li, H. Wang, Y. Shang, B. Li, W. Guo, L. Zhang, J. Mater. Chem. C 2016, 4, 7724.
- [61] J. Yuan, S. Yao, P. Poulin, in *Polymer Nanocomposites: Electrical and Thermal Properties*, (Eds: X. Huang, C. Zhi), Springer International Publishing, Cham 2016, 3.
- [62] K. Shehzad, A. A. Hakro, Y. Zeng, S.-H. Yao, Y. Xiao-Hong, M. Mumtaz, K. Nadeem, N. S. Khisro, Z.-M. Dang, Applied Nanoscience 2015, 5, 969.
- [63] L. Zhang, W. Wang, X. Wang, P. Bass, Z.-Y. Cheng, Appl. Phys. Lett. 2013, 103, 232903.
- [64] M. Molberg, D. Crespy, P. Rupper, F. Nüesch, J.-A. E. Månson, C. Löwe, D. M. Opris, Adv. Funct. Mater. 2010, 20, 3280.
- [65] S.-Q. Wu, J.-W. Wang, J. Shao, L. Wei, K. Yang, H. Ren, ACS Appl. Mater. Interfaces 2017, 9, 28887.

- [66] C. C. Ku, R. Liepins, *Electrical Properties of Polymers: Chemical Principles*, Hanser, 1987.
- [67] D. F. Miranda, S. Zhang, J. Runt, Macromolecules 2017, 50, 8083.
- [68] N. M. Putintsev, D. N. Putintsev, Russ. J. Phys. Chem. 2006, 80, 1949.
- [69] J. Mao, T. Li, Y. Luo, J. Mater. Chem. C 2017, 5, 6834.
- [70] S. Yilmaz, W. Wirges, S. Bauer-Gogonea, S. Bauer, R. Gerhard-Multhaupt, F. Michelotti, E. Toussaere, R. Levenson, J. Liang, J. Zyss, Appl. Phys. Lett. 1997, 70, 568.
- [71] X. Yuan, T. C. M. Chung, Appl. Phys. Lett. 2011, 98, 062901.
- [72] T. Chen, J. Qiu, K. Zhu, J. Li, J. Wang, S. Li, X. Wang, J. Phys. Chem. B 2015, 119, 4521.
- [73] S. J. Dunki, M. Tress, F. Kremer, S. Y. Ko, F. A. Nuesch, C.-D. Varganici, C. Racles, D. M. Opris, RSC Adv. 2015, 5, 50054.
- [74] B. Marciniec, *Hydrosilylation: a comprehensive review on recent advances*, Vol. 1, Springer Science & Business Media, 2008.
- [75] J. E. Mark, *Polymer Data Handbook (2nd Edition)*, Oxford University Press, 2009.
- [76] B. Marciniec, J. Guliński, L. Kopylova, H. Maciejewski, M. Grundwald-Wyspiańska, M. Lewandowski, Appl. Organomet. Chem. 1997, 11, 843.
- [77] J. G. Matisons, A. Provatas, Macromolecules 1994, 27, 3397; X. Coqueret, A. Lablache-Combier, C. Loucheux, Eur. Polym. J. 1988, 24, 1137.
- [78] Z. Zhu, A. G. Einset, C.-Y. Yang, W.-X. Chen, G. E. Wnek, Macromolecules 1994, 27, 4076.
- [79] X. Coqueret, G. Wegner, Organometallics 1991, 10, 3139; L. C. Chien, L. G. Cada, Macromolecules 1994, 27, 3721.
- [80] M. Dascalu, S. J. Dunki, J.-E. Q. Quinsaat, Y. S. Ko, D. M. Opris, RSC Adv. 2015, 5, 104516.

- [81] F. B. Madsen, L. Yu, A. E. Daugaard, S. Hvilsted, A. L. Skov, RSC Adv. 2015, 5, 10254.
- [82] C. Racles, V. Cozan, A. Bele, M. Dascalu, Des. Monomers Polym. 2016, 19, 496.
- [83] C. Racles, M. Alexandru, A. Bele, V. E. Musteata, M. Cazacu, D. M. Opris, RSC Adv. 2014, 4, 37620.
- [84] M. Böhm, W. v. Soden, W. Heinrich, A. A. Yehia, Colloid. Polym. Sci. 1987, 265, 295.
- [85] C. Racles, C. Maria, F. Beatrice, M. O. Dorina, Smart Mater. Struct. 2013, 22, 104004.
- [86] C. Racles, A. Bele, M. Dascalu, V. E. Musteata, C. D. Varganici, D. Ionita, S. Vlad, M. Cazacu, S. J. Dunki, D. M. Opris, RSC Adv. 2015, 5, 58428.
- [87] P. J. Collings, M. Hird, *Introduction to Liquid Crystals: Chemistry and Physics*, CRC Press, 1997.
- [88] A. L. Skov, L. Yu, Adv. Eng. Mater., 1700762.
- [89] B. Kussmaul, S. Risse, G. Kofod, R. Waché, M. Wegener, D. N. McCarthy, H. Krüger, R. Gerhard, Adv. Funct. Mater. 2011, 21, 4589.
- [90] K. Björn, R. Sebastian, W. Michael, K. Guggi, K. Hartmut, Smart Mater. Struct. 2012,21, 064005.
- [91] S. Risse, B. Kussmaul, H. Kruger, G. Kofod, RSC Adv. 2012, 2, 9029.
- [92] C. Zou, J. C. Fothergill, S. W. Rowe, IEEE Trans. Dielectr. Electr. Insul. 2008, 15, 106.
- [93] A. Bele, M. Cazacu, C. Racles, G. Stiubianu, D. Ovezea, M. Ignat, Adv. Eng. Mater. 2015, 17, 1302.
- [94] M. Tian, H. Yan, H. Sun, L. Zhang, N. Ning, RSC Adv. 2016, 6, 96190.
- [95] Z. Hordyjewicz-Baran, L. You, B. Smarsly, R. Sigel, H. Schlaad, Macromolecules 2007, 40, 3901.
- [96] J. Justynska, Z. Hordyjewicz, H. Schlaad, Polymer 2005, 46, 12057.
- [97] N. ten Brummelhuis, C. Diehl, H. Schlaad, Macromolecules 2008, 41, 9946.

- [98] S. J. Dunki, F. A. Nuesch, D. M. Opris, J. Mater. Chem. C 2016, 4, 10545.
- [99] S. J. Dunki, E. Cuervo-Reyes, D. M. Opris, Polym. Chem. 2017, 8, 715.
- [100] M. Node, K. Kumar, K. Nishide, S.-i. Ohsugi, T. Miyamoto, Tetrahedron Lett. 2001, 42, 9207.
- [101] J. Bai, Z. Shi, J. Yin, M. Tian, Polym. Chem. 2014, 5, 6761.
- [102] X. Huang, C. Zhi, P. Jiang, D. Golberg, Y. Bando, T. Tanaka, Adv. Funct. Mater. 2013, 23, 1824.
- [103] N. Suzuki, S. Kiba, Y. Yamauchi, Microporous Mesoporous Mater. 2011, 138, 123.
- [104] K. Sethuraman, M. R. Vengatesan, T. Lakshmikandhan, M. Alagar, High Perform. Polym. 2016, 28, 340.
- [105] F. B. Madsen, I. Dimitrov, A. E. Daugaard, S. Hvilsted, A. L. Skov, Polym. Chem. 2013, 4, 1700.
- [106] F. B. Madsen, L. Yu, A. E. Daugaard, S. Hvilsted, A. L. Skov, Polymer 2014, 55, 6212.
- [107] J. O. Bostrom, E. Marsden, R. N. Hampton, U. Nilsson, IEEE Electr. Insul. M. 2003, 19, 6.
- [108] F. B. Madsen, A. E. Daugaard, S. Hvilsted, M. Y. Benslimane, A. L. Skov, Smart Mater. Struct. 2013, 22, 104002.
- [109] S. Li, G. Yin, G. Chen, J. Li, S. Bai, L. Zhong, Y. Zhang, Q. Lei, IEEE Trans. Dielectr. Electr. Insul. 2010, 17, 1523.
- [110] J. Su, J. S. Harrison, T. S. Clair, "Novel polymeric elastomers for actuation", presented at *ISAF 2000. Proceedings of the 2000 12th IEEE International Symposium on Applications of Ferroelectrics (IEEE Cat. No.00CH37076)*, 2000, 2000.
- [111] A. M. Menzel, Phys. Rep. 2015, 554, 1.
- [112] P. G. de Gennes, J. Prost, *The Physics of Liquid Crystals*, Clarendon Press, 1995.

- [113] F. Brömmel, D. Kramer, H. Finkelmann, in *Liquid Crystal Elastomers: Materials and Applications*, Vol. 250 (Ed: W. H. de Jeu), Springer Berlin Heidelberg, Berlin, Heidelberg 2012, 1.
- [114] R. Wei, Y. He, X. Wang, RSC Adv. 2014, 4, 58386.
- [115] C. Loubser, C. Imrie, P. H. van Rooyen, Adv. Mater. 1993, 5, 45.
- [116] Y. Yusuf, Y. Ono, Y. Sumisaki, P. E. Cladis, H. R. Brand, H. Finkelmann, S. Kai, Phys. Rev. E 2004, 69, 021710.
- [117] C. Ohm, M. Brehmer, R. Zentel, Adv. Mater. 2010, 22, 3366.
- [118] J. Küpfer, H. Finkelmann, Makromol. Chem., Rapid Commun 1991, 12, 717.
- [119] H. Finkelmann, G. Rehage, Makromol. Chem., Rapid Commun 1980, 1, 733.
- [120] H. Jiang, C. Li, X. Huang, Nanoscale 2013, 5, 5225.
- [121] P. Beyer, L. Braun, R. Zentel, Macromol. Chem. Phys. 2007, 208, 2439.
- [122] J. Lub, D. J. Broer, N. van den Broek, Liebigs Ann. 1997, 1997, 2281.
- [123] C. Zhang, D. Wang, J. He, M. Liu, G.-H. Hu, Z.-M. Dang, Polym. Chem. 2014, 5, 2513.
- [124] J. Küupfer, H. Finkelmann, Macromol. Chem. Phys. 1994, 195, 1353.
- [125] T. C. Lubensky, R. Mukhopadhyay, L. Radzihovsky, X. Xing, Phys. Rev. E 2002, 66, 011702.
- [126] W. Lehmann, H. Skupin, C. Tolksdorf, E. Gebhard, R. Zentel, P. Krüger, M. Lösche, F. Kremer, Nature 2001, 410, 447.
- [127] K. Matyjaszewski, Macromolecules 2012, 45, 4015.
- [128] K. Min, H. Gao, K. Matyjaszewski, J. Am. Chem. Soc. 2005, 127, 3825; H. Ding, S. Park,
 M. Zhong, X. Pan, J. Pietrasik, C. J. Bettinger, K. Matyjaszewski, Macromolecules 2016, 49,
 6752.
- [129] P. G. de Gennes, C. R. Seances Acad. Sci., Ser. B 1975, 281, 101.

- [130] G. H. F. Bergmann, H. Finkelmann, V. Percec, M. Zhao, Macromol. Rapid Commun. 1997, 18, 353.
- [131] F. Greco, V. Domenici, A. Desii, E. Sinibaldi, B. Zupancic, B. Zalar, B. Mazzolai, V. Mattoli, Soft Matter 2013, 9, 11405.
- [132] S. Fu, H. Zhang, Y. Zhao, J. Mater. Chem. C 2016, 4, 4946.
- [133] Y. Yang, W. Zhan, R. Peng, C. He, X. Pang, D. Shi, T. Jiang, Z. Lin, Adv. Mater. 2015, 27, 6376.
- [134] C. Zhang, D. Wang, J. He, T. Liang, G.-H. Hu, Z.-M. Dang, Polym. Adv. Technol. 2014, 25, 920.
- [135] H. E. Hofmann, Ind. Eng. Chem. 1932, 24, 135.
- [136] W.-H. Huang, P.-Y. Chen, S.-H. Tung, Macromolecules 2012, 45, 1562.
- [137] L. Zhang, D. Wang, P. Hu, J.-W. Zha, F. You, S.-T. Li, Z.-M. Dang, J. Mater. Chem. C 2015, 3, 4883.
- [138] C. Huang, Q. M. Zhang, Adv. Mater. 2005, 17, 1153.
- [139] H. Stoyanov, M. Kollosche, D. N. McCarthy, G. Kofod, J. Mater. Chem. 2010, 20, 7558.
- [140] B. K. Paul, R. K. Mitra, J. Colloid Interface Sci. 2006, 295, 230.
- [141] A. Epstein, B. S. Wildi, J. Chem. Phys. 1960, 32, 324.
- [142] C. G. Hardy, M. S. Islam, D. Gonzalez-Delozier, J. E. Morgan, B. Cash, B. C. Benicewicz, H. J. Ploehn, C. Tang, Chem. Mater. 2013, 25, 799.
- [143] J. Casanovas, M. Canales, C. A. Ferreira, C. Alemán, J. Phys. Chem. A 2009, 113, 8795.
- [144] G. Yang, W. Hou, X. Feng, X. Jiang, J. Guo, Int. J. Quantum Chem 2008, 108, 1155.
- [145] N. Wang, C. Cui, H. Guo, B. Chen, X. Zhang, Science China Technological Sciences 2017.
- [146] D. McCoul, S. Rosset, N. Besse, H. Shea, Smart Mater. Struct. 2017, 26, 025015.

- [147] L. Qin, J. Cao, Y. Tang, J. Zhu, Journal of Applied Mechanics 2018, 85, 051001.
- [148] F. A. Mohd Ghazali, C. K. Mah, A. AbuZaiter, P. S. Chee, M. S. Mohamed Ali, Sensors and Actuators A: Physical 2017, 263, 276.
- [149] J. Shintake, S. Rosset, B. Schubert, D. Floreano, H. Shea, Adv. Mater. 2016, 28, 231.
- [150] R. K. Katzschmann, A. D. Marchese, D. Rus, in *Experimental Robotics: The 14th International Symposium on Experimental Robotics*, (Eds: M. A. Hsieh, O. Khatib, V. Kumar), Springer International Publishing, Cham 2016, 405.
- [151] R. F. Shepherd, F. Ilievski, W. Choi, S. A. Morin, A. A. Stokes, A. D. Mazzeo, X. Chen, M. Wang, G. M. Whitesides, Proceedings of the National Academy of Sciences 2011, 108, 20400.
- [152] S. Bauer, S. Bauer-Gogonea, I. Graz, M. Kaltenbrunner, C. Keplinger, R. Schwödiauer, Adv. Mater. 2014, 26, 149.
- [153] D. Rus, M. T. Tolley, Nature 2015, 521, 467.
- [154] C. Graf, J. Maas, D. Schapeler, in *Conference on Electroactive Polymer Actuators and Devices (EAPAD) 2010*, Vol. 7642, Spie-Int Soc Optical Engineering, San Diego, CA 2010.
- [155] P. Zanini, J. Rossiter, M. Homer, Smart Mater. Struct. 2017, 26, 035037.
- [156] C. Jean-Mistral, S. Basrour, J.-J. Chaillout, in *SPIE Smart Structures and Materials + Nondestructive Evaluation and Health Monitoring*, Vol. 6927, SPIE, 2008, 10.
- [157] T. McKay, B. O'Brien, E. Calius, I. Anderson, Smart Mater. Struct. 2010, 19, 055025.
- [158] T. McKay, B. O'Brien, E. Calius, I. Anderson, Appl. Phys. Lett. 2010, 97, 062911.
- [159] T. G. McKay, B. M. O'Brien, E. P. Calius, I. A. Anderson, Appl. Phys. Lett. 2011, 98, 142903.
- [160] S. J. A. Koh, X. Zhao, Z. Suo, Appl. Phys. Lett. 2009, 94, 262902.
- [161] T. A. Gisby, S. Xie, E. P. Calius, I. A. Anderson, in *SPIE Smart Structures and Materials*+ *Nondestructive Evaluation and Health Monitoring*, Vol. 7287, SPIE, 2009, 12.

- [162] G. J. Lin, K. S. Wang, Adv. Mater. Res. 2014, 1039, 415.
- [163] G. Moretti, G. P. R. Papini, M. Righi, D. Forehand, D. Ingram, R. Vertechy, M. Fontana, Smart Mater. Struct. 2018, 27, 035015.
- [164] C. Racles, M. Ignat, A. Bele, M. Dascalu, D. Lipcinski, M. Cazacu, Smart Mater. Struct. 2016, 25, 085024.
- [165] P. Jean, A. Wattez, G. Ardoise, C. Melis, R. V. Kessel, A. Fourmon, E. Barrabino, J. Heemskerk, J. P. Queau, "Standing wave tube electro active polymer wave energy converter", presented at *SPIE Smart Structures and Materials + Nondestructive Evaluation and Health Monitoring*, 2012.
- [166] A. Lasheras, J. Gutiérrez, S. Reis, D. Sousa, M. Silva, P. Martins, S. Lanceros-Mendez, J.
 M. Barandiarán, D. A. Shishkin, A. P. Potapov, Smart Mater. Struct. 2015, 24, 065024; J. Song,
 G. Zhao, B. Li, J. Wang, Heliyon 2017, 3, e00377; S. Park, Y. Kim, H. Jung, J.-Y. Park, N. Lee, Y.
 Seo, Scientific Reports 2017, 7, 17290.

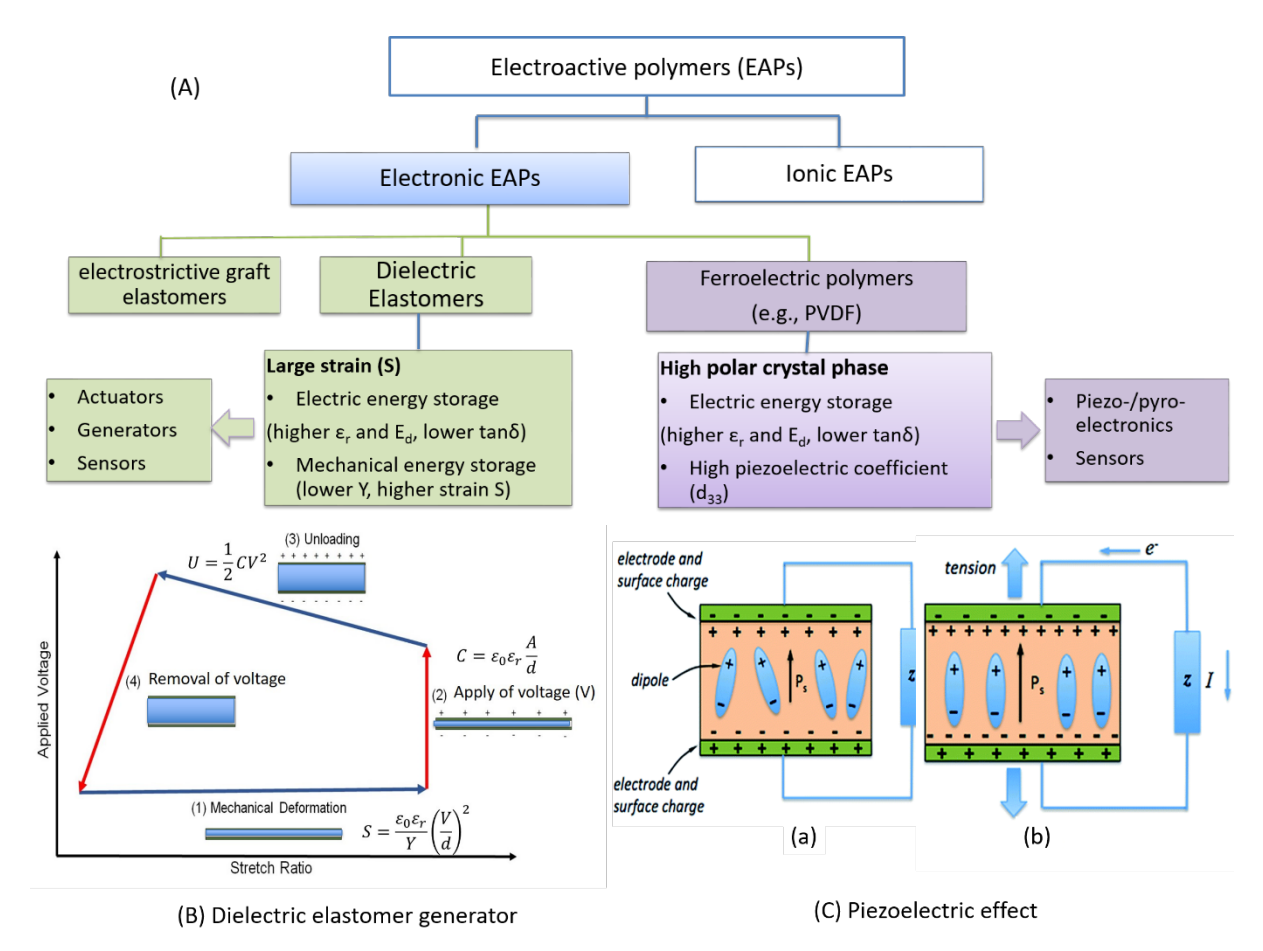


Figure 1. (A) Classification of electroactive polymers and the working mechanism of (B) dielectric elastomers and (C) ferroelectric polymers

Figure 2. Macromolecular structures of some dielectric elastomers and semi-crystalline polymers: SBS; SEBS; PDMS; EPDM, natural rubber, nitrile-butadiene rubber (NBR) and the semi-crystalline polymers of poly(lactic acid), nylon-11, PVDF, P(VDF-HFP) and P(VDF-TrFE-CFE)

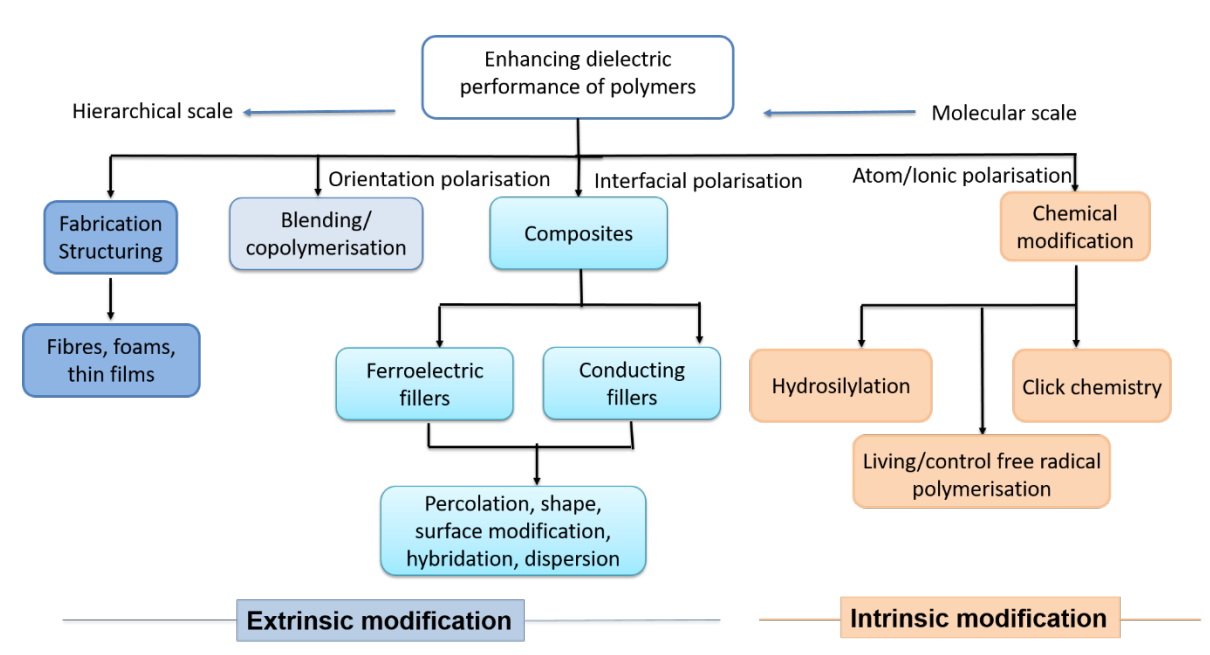


Figure 3. Modification methods of dielectric elastomers for enhancing electromechanical properties

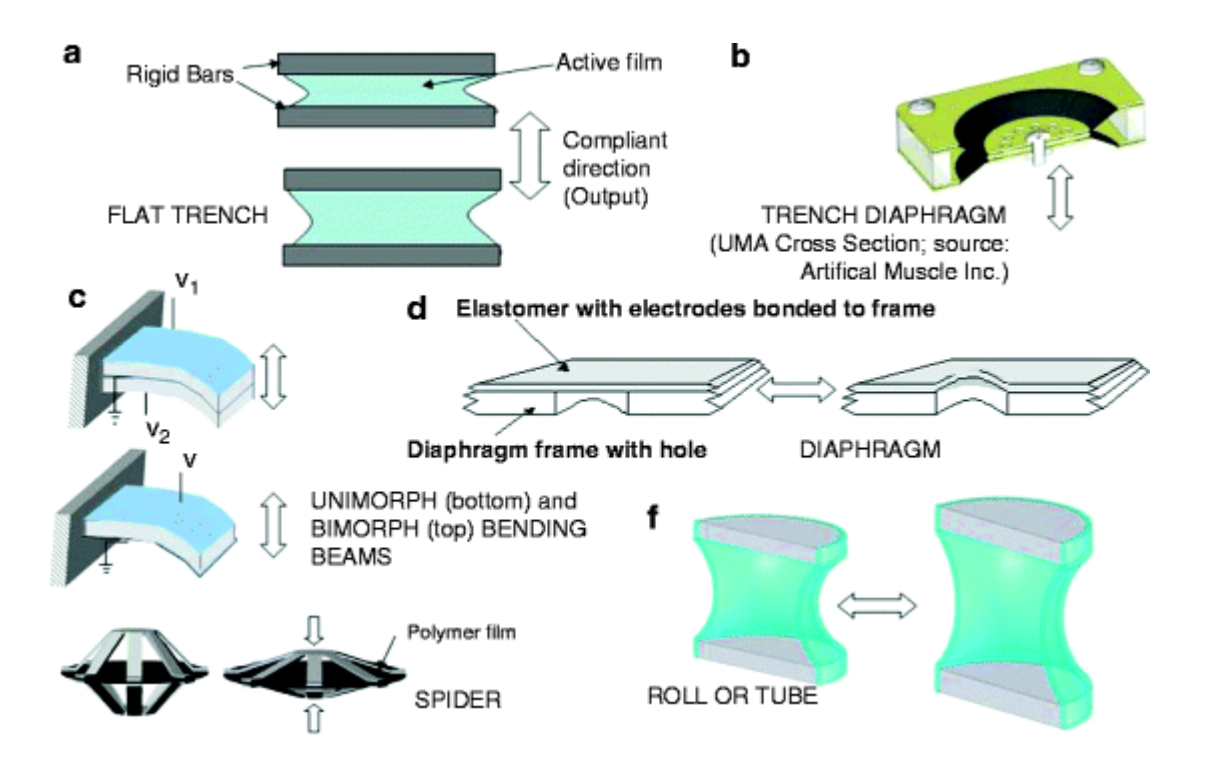


Figure 4. Different dielectric elastomer device configurations for varying applications. Reprinted with permission from Kornbluh et al^[39]. Copyright 2013, Springer Nature

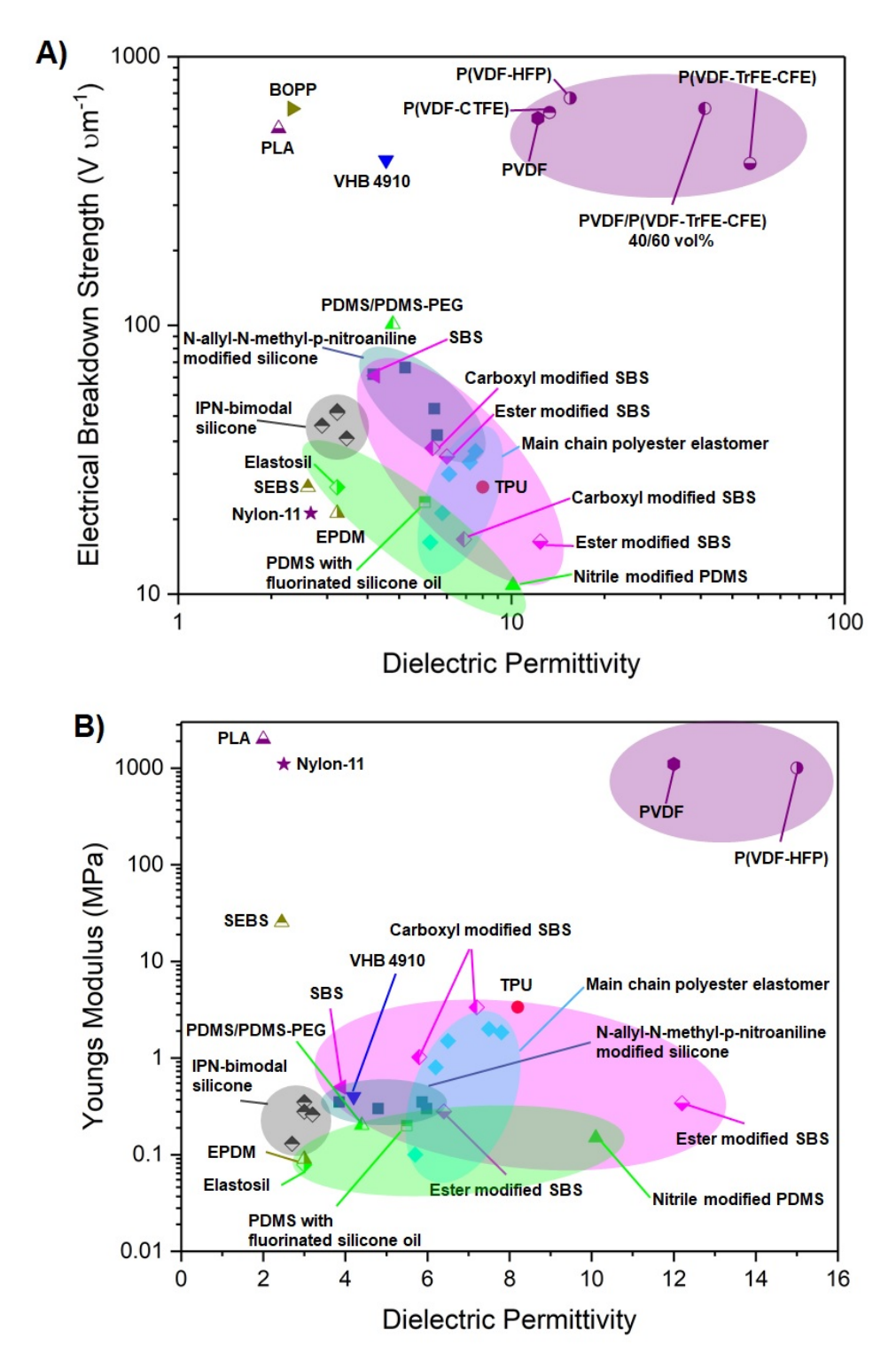


Figure 5. Comparison between (a) dielectric permittivity and electrical breakdown strength, and (b) dielectric permittivity and Young's modulus, of different materials

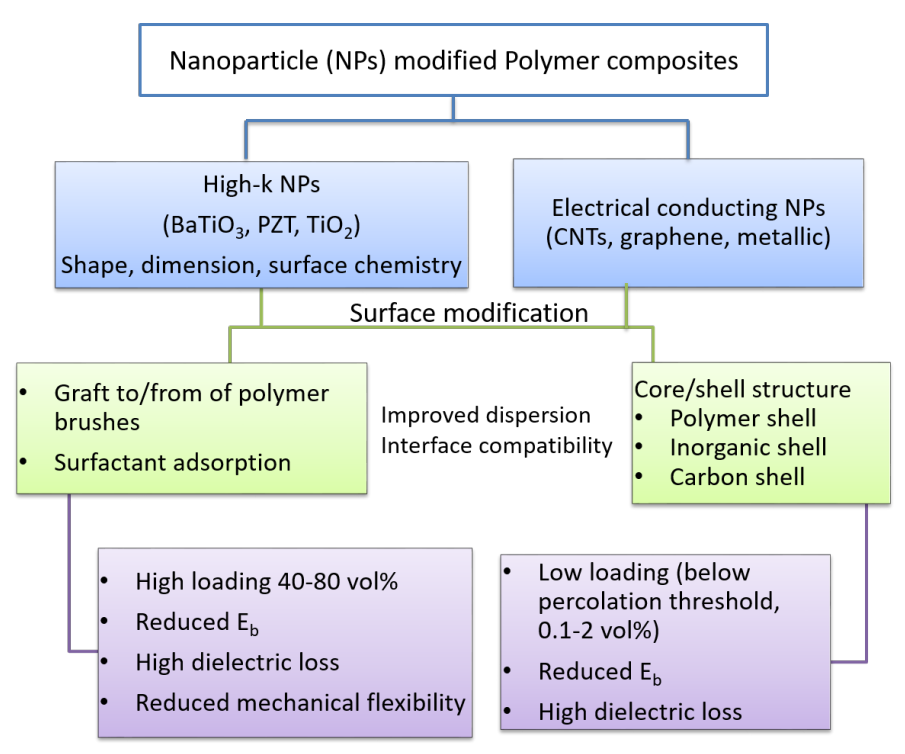


Figure 6. Fabrication of high-permittivity extrinsic polymer composites using nanoparticles (NPs)

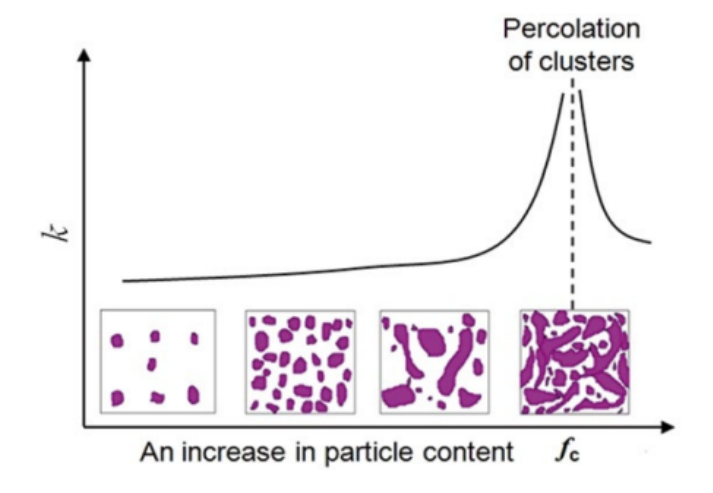


Figure 7. Changes in dielectric permittivity on approaching the percolation threshold as the content of filler in increased. Reprinted with permission from Yuan et al^[61]. Copyright 2016, Springer Nature

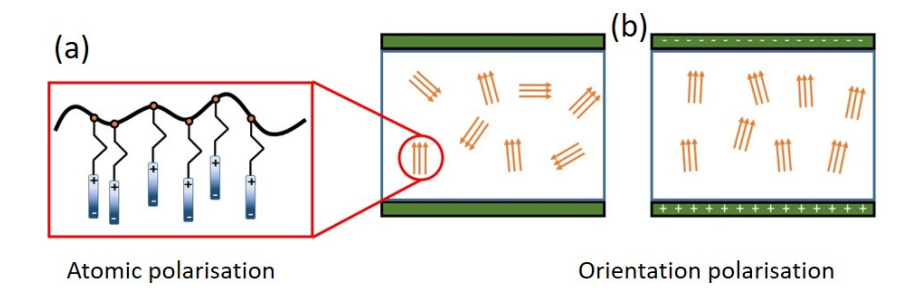


Figure 8. Schematic of a) atomic polarisation and b) orientation polarisation within a polymer

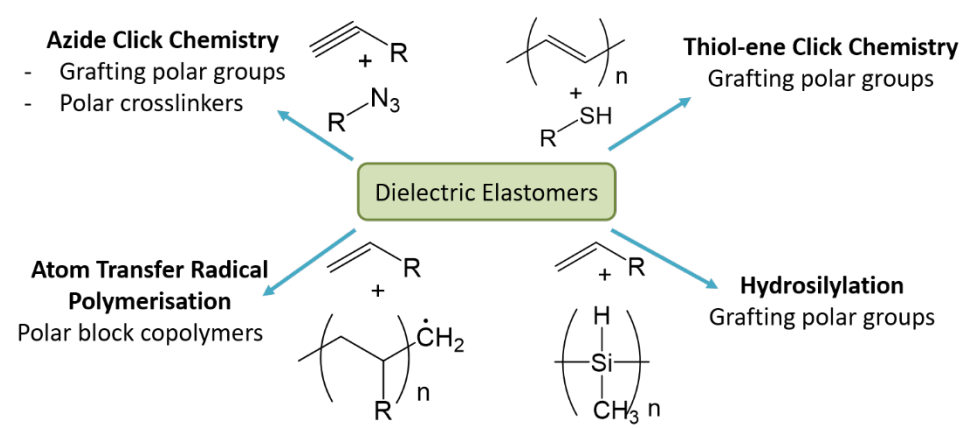


Figure 9. The main chemical modification reactions for enhancing the polarity of dielectric elastomers

$$\begin{array}{c} CH_{3} \\ H_{3}C \\ \hline \\ CH_{3} \\ CH_{3} \\ \hline \\ CH_{3} \\ CH_{4} \\ CH_{5} \\ CH_{5$$

Figure 10. General reaction scheme and conditions for hydrosilylation of silicone based polymers

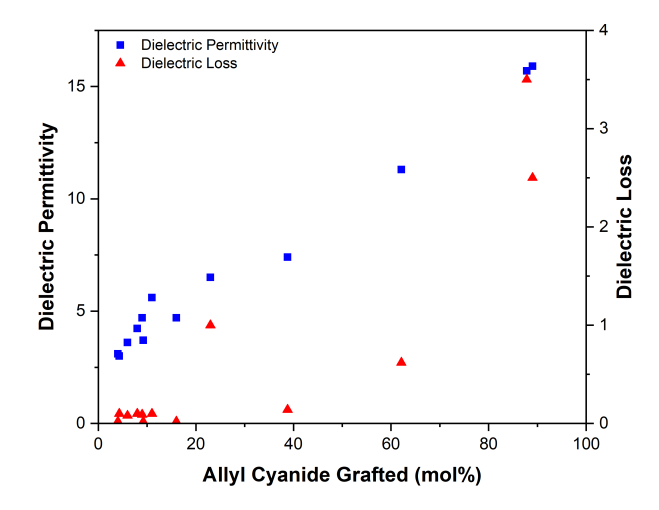


Figure 11. Correlation between allyl cyanide content and the increase in ε_r and ε' .

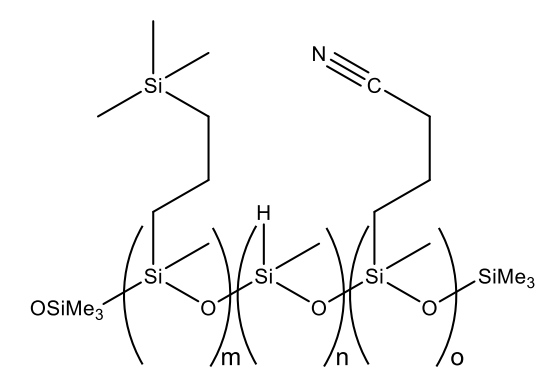


Figure 12. Chemical structure of CNATS-993 used as a filler in PDMS

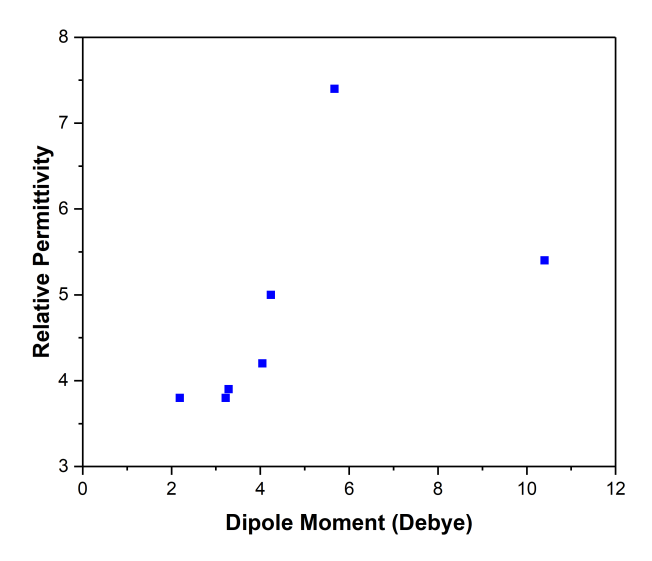


Figure 13. Graph showing the weak correlation between dipole moment of organic dipole grafted and the permittivity of the elastomer.

Figure 14. Thiol-ene click reaction scheme for modification of SBS in which there are four different ways the thiol can bond

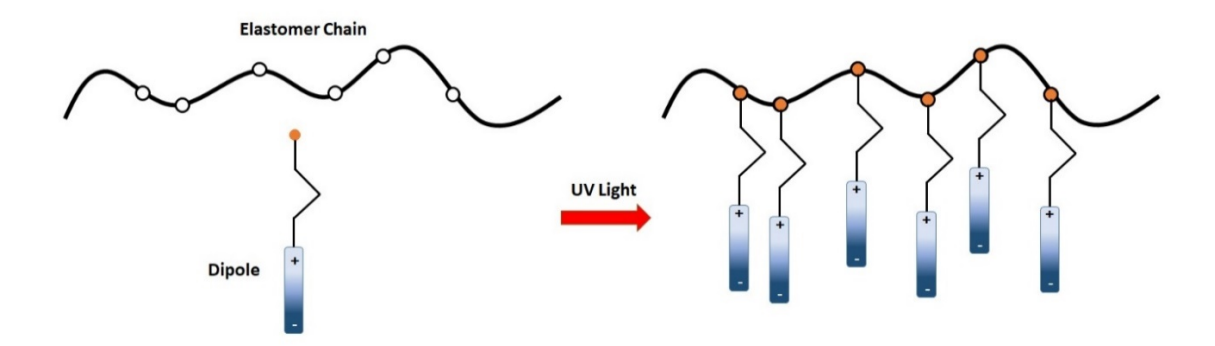


Figure 15. Dipoles can simply 'click' and attach to elastomer chains via click chemistry

$$\begin{array}{c} R \\ O \\ O \\ R \end{array}$$

$$\begin{array}{c} Cul, Et_3N \\ 40^{\circ}C, 17h \end{array}$$

Figure 16. Reaction scheme for copper(I) catalysed alkyne-azide cycloaddition reaction to

form a 1,4-disubstituted product

Aniline tetramer

Figure 17 Examples of Azo (top), ferrocenyl (middle) and aniline (bottom) containing

mesogens

Figure 18. Reaction scheme for Atom Transfer Radical Polymerisation (ATRP)

Figure 19. Chemical structure of 11CBMA

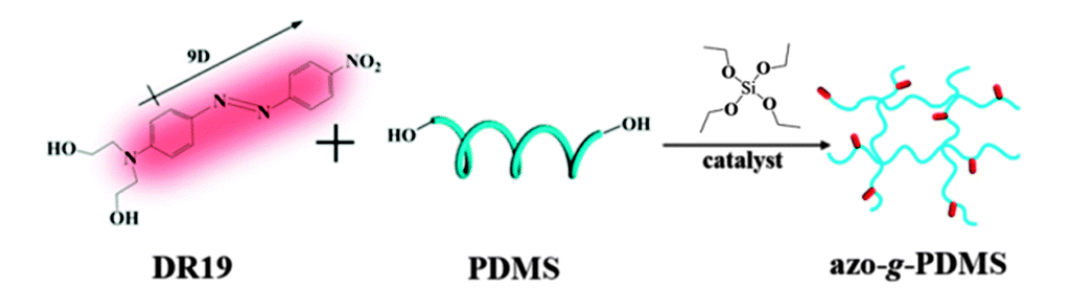


Figure 20. Reaction scheme for grafting DR19 to PDMS. Reprinted with permission from Zhang et al^[137]. Copyright 2015, Royal Society of Chemistry

Figure 21. Structure of PU-g-CuPc-PANI. Reprinted with permission from Huang et al^[138]. Copyright 2005, John Willey and Sons

Figure 22. Structure of oligoaniline end capped polystyrene

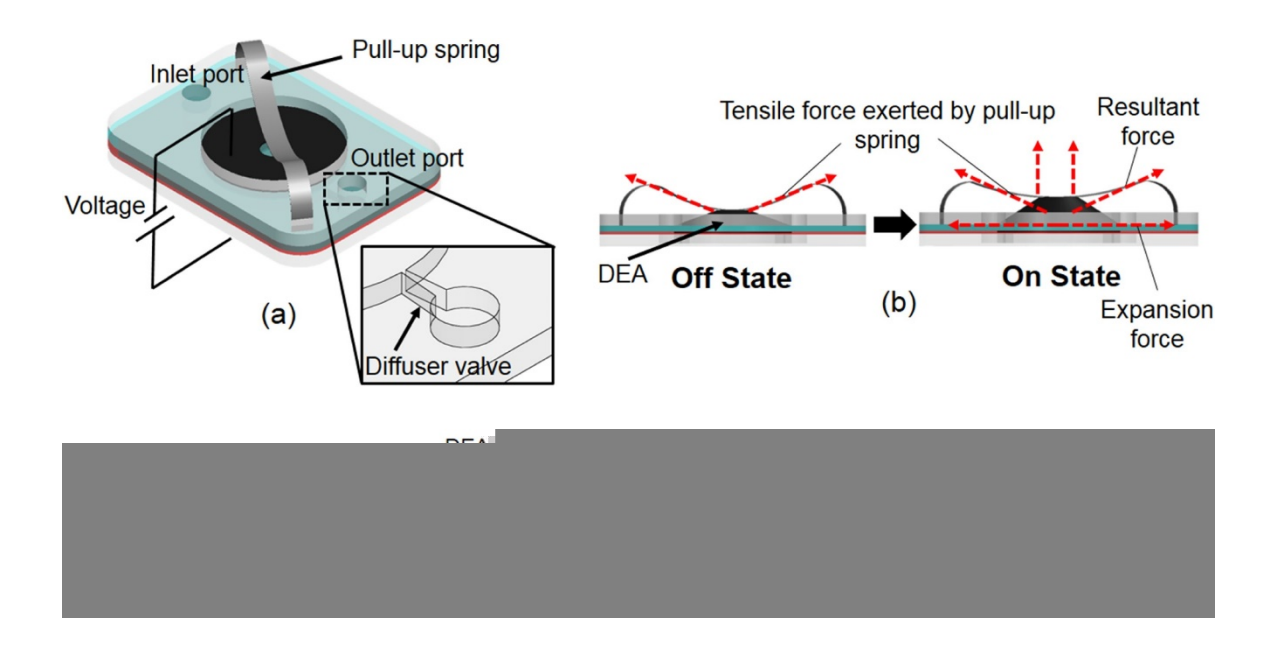


Figure 23. Microfluidic pump set-up using the change in shape of a dielectric elastomer in actuation mode under an applied voltage to provide the pumping motion. Reprinted with permission from Ghazali et al^[148]. Copyright 2017, Elsevier

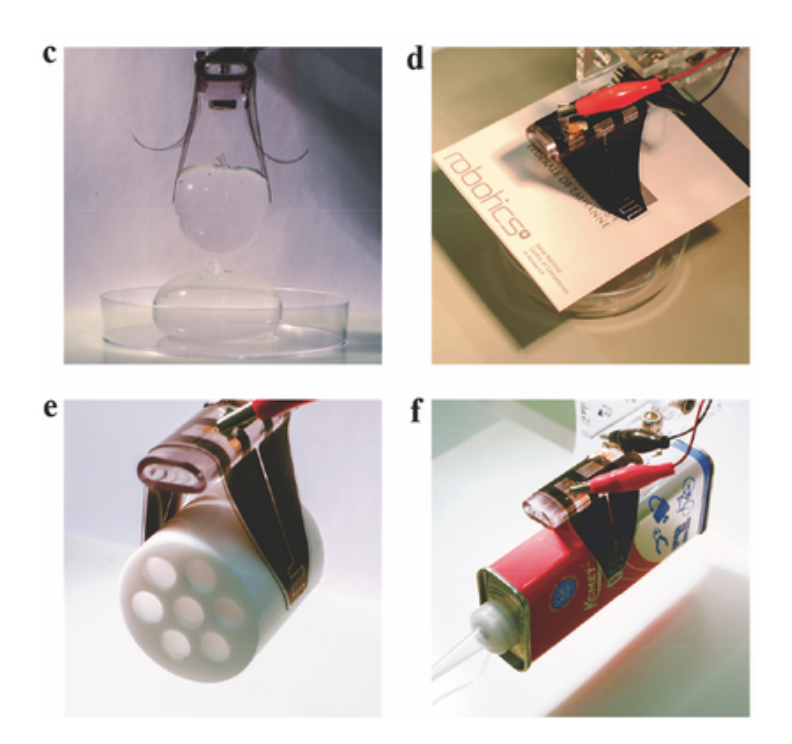


Figure 24. Schematic design of the actuating soft gripper and demonstration of a soft gripper successfully picking up a variety of objects including (a) a thin membraned water balloon, (b) flat paper, (c) Teflon tube and (d) oil can. Reprinted with permission from Shintake et al^[149]. Copyright 2015, John Willey and Sons

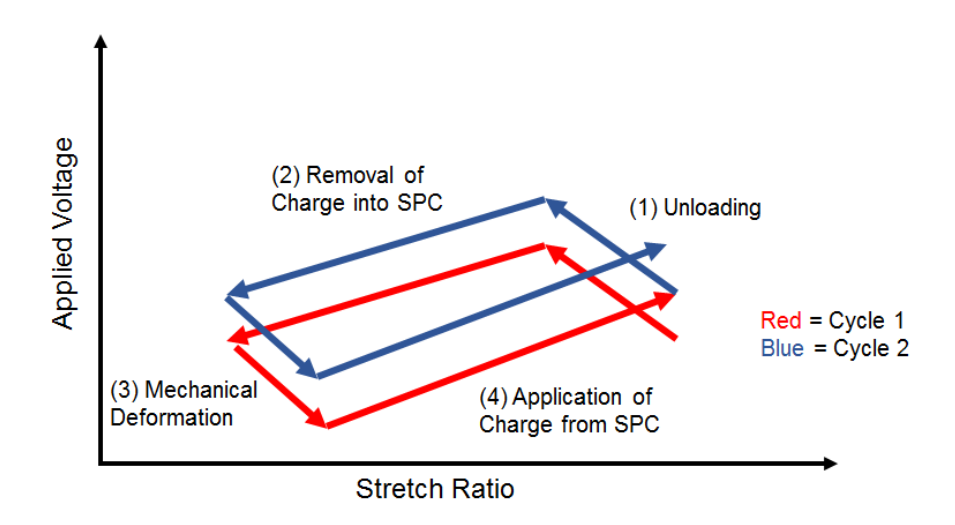


Figure 25. Working mechanism of a device using self-priming circuits for voltage enhancement

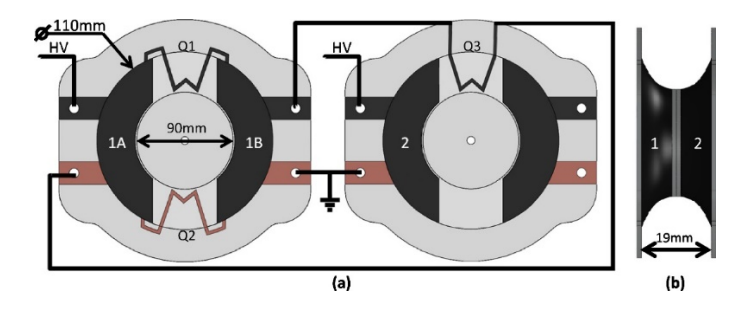


Figure 26. Dielectric elastomer generator with piezoresistive switches. Reprinted with permission from McKay et al^[159]. Copyright 2011, AIP Publishing LLC

Table 1. Comparison of dielectric and mechanical properties for materials of interest

Material	$\boldsymbol{arepsilon}_r$	arepsilon'	E_b	d_{33}	Τ	Υ	λ_{max}	Figure of	Figure of
			[V	[pC	[MPa]	[MPa]	[%]	Merit	Merit
			μm ⁻¹]	N^{-1}]				(actuation)	(generation)
SBS ^[24]	3.90	3.0×10 ⁻⁴	65	-	16.4	5.0×10 ⁻¹	1350	8.7	0.0039
SEBS ^[25]	2.45	5.0×10 ⁻⁴	25	-	27.1	25.4	518	0.016	0.00037
PDMS ^[26, 27]	2.50	2.0×10 ⁻⁴	80	-	1.1	9.0×10 ⁻¹	200	4.7	0.0038
EPDM ^[28]	3.00	1.0×10 ⁻³	20	-	1.0	9.0×10 ⁻²	600	3.5	0.00029
PVDF ^[29, 30]	12	1.8×10 ⁻²	590	20	290	1.1×10^{3}	50	1	1

VHB 4905 ^{[24, 31} 32]	_	-	218	-	0.8	0.4	500	143.9	0.052
Nylon- 11 ^[33]	2.50	4.0×10 ⁻³	20	4.1	44	1.1×10 ³	320	0.00024	0.00024
Poly(laction acid) ^[34]	2.00	2×10 ⁻²	540	3.1	60	2×10 ³	40	0.077	0.14
BaTiO ₃ ^{[35,}	1700	1	38	191	59.0	1.2×10 ⁵	-	0.0054	0.59
PZT ^[36, 37]	1300	5.0×10 ⁻²	120	289	83.0	6.3×10 ⁴	-	0.078	4.5

 Table 2. Electrical properties of PVDF, PVDF copolymers and PDMS blends

Polymers	ε_r (@1	E_b (MV/m)	arepsilon'	U_e (J/cm ³) Figure of	Figure of
	kHz)				Merit	Merit
					(Actuation)	(Generation)
PVDF ^[30]	12	590		2.4	1	1
P(VDF-CTFE) ^[41]	13	620		25	-	1.2
P(VDF-HFP) ^[42]	15	700		25	1.9	1.8
P(VDF-TrFE-CFE) ^[43]	52	400		10	-	2.0
PVDF/P (VDF-TrFE-CFE)	38	640	5×10 ⁻²	19.6	-	3.7
(40/60 vol%) blend ^[40]						
PVDF-St (39 wt%) ^[44]	80				-	-
P(VDF-co-2-	45		2.0×10 ⁻³		-	-
hexaethylmethacrylate) ^[45]						
PVDF+PA11 ^[46]	188		1.37		-	-
BOPP ^[47]	2.2	> 640	<0.02	1~2	-	0.22
PDMS-PEG ^[48]	5		5×10 ⁻²		-	-
PDMS/PDMS-PEG ^[48]	4.4	101	5×10 ⁻²		58.2	0.011
PDMS+fluorinated silicone	5.5	22	8×10 ⁻²		3.5	0.00064
oil ^[49]						